Normal and Superconducting Properties of the High-T_c Oxides. The Van Hove Scenario

A. Bechlaghem*

Faculté des Sciences de la Nature et de la Vie, Université d'Oran 1 Ahmed Ben Bella, Algeria

Abstract: In this review, we study the normal and superconducting properties of the high-T_c cuprate superconductors. We provide an overview of general concepts relevant to these compounds. We review the experimental results of the pseudogap, the electrical resistivity and the Hall constant which are considered as relevant to cuprates in understanding their normal state. The competition between SDW, CDW and superconductivity is also discussed in this work. The van Hove singularity (VHS) appears to play a crucial role in these new superconductors, particularly since experimental studies have found that the Fermi level ε_F lies close to the VHS in most of high-T_c cuprates. After a description of the van Hove singularity model, we evaluate and analyze the major parameters of these compounds. General expressions of the superconducting gap ratio R and the isotope coefficient α are obtained in the van Hove scenario and discussed in more detail. Our theoretical results are in qualitative agreement with experimental results.

Keywords: Superconductivity, Van Hove singularity, Magnetic correlations, Penetration depth, Superconducting gap, Pseudogap, Electrical resistivity, Hall constant, Spin density waves, Charge density waves, Jahn-Teller effect, Coherence length, Effective mass, Superconducting gap ratio, Isotope effect.

1. INTRODUCTION

Since the discovery of superconductivity in lanthanum compound by Bednorz and Muller [1], there is an intense research both experimentally and theoretically to understand the origin of superconductivity in this compound. In the seven years following this discovery, a series of copper oxides are discovered and the critical temperature has reached values of order of 135 K. During this period various models and theories have been proposed to explain the mechanism of superconductivity in these compounds [2-10].

These high-T_c oxide superconductors are divided into two principal groups:

- the hole-doped cuprates: such lanthanum compound $La_{2-x}Sr_xCuO_4$ (LSCO) with $T_c^{\max} = 39$ K for $x = 0.15$; the yttrium compound $YBa_2Cu_3O_{6+x}$ (YBCO) with $T_c^{\max} = 92$ K for $x = 1$; the bismuth compounds $Bi_mSr_2Ca_{n-1}Cu_nO_{2n+m+2+x}$ $(m2(n-1)n, n = 2,3)$: the compound Bi-2212 *i.e* $Bi_2Sr_2CaCu_2O_8$ with $T_c^{\max} = 86$ K and Bi-2223 *i.e* $Bi_2Sr_2Ca_2Cu_3O_{10}$ with $T_c^{\max} = 110$ K; the thallium compounds $Tl_mBa_2Ca_{n-1}Cu_nO_{2n+m+2}$ $(m2(n-1)n, n = 2,3)$: the compound Th-2212 with $T_c^{\max} = 100$ K and Th-2223 with $T_c^{\max} = 125$ K; the mercury compounds $HgBa_2Ca_{n-1}Cu_nO_{2n+x+2}$ $(Hg-12(n-1)n, n = 1,2,3)$. Samples of optimally doped Hg-1201, Hg-1212, and Hg-1223 have critical temperature $T_c^{\max} = 96$ K, 123 K and 135 K respectively,
- the electron-doped cuprates: such neodymium compound $Nd_{2-x}Ce_xCuO_4$ (NCCO) with $T_c^{\max} = 22$ K for $x = 0.15$; $Pr_{2-x}CuO_4$ (PCCO) with $T_c^{\max} = 19$ K for $x = 0.15$; $Pr_{1-x}LaCe_xCuO_4$ (PLCCO) with $T_c^{\max} = 24-26$ K for $x = 0.11-0.12$.

These compounds are doped materials, with $T_c(x)$ strongly depending on carrier concentration x. In low doping regime, the high-T_c oxides are antiferromagnetic insulators. Upon concentration doping, the antiferromagnetic order rapidly disappears and the system becomes a superconductor [11-16]. In these compounds the magnetic correlations persist and are still present at optimal doping x_{op} [11, 13, 14].

The superconducting transition temperature $T_c(x)$ increases with doping and reaches its maximum at optimal doping x_{op}. From the optimal doping, $T_c(x)$ decreases with x and it is suppressed at higher x values. The superconducting transition temperature $T_c(x)$ can be expressed as: $T_c(x)/T_c^{\max} = 1-\left((x_{op}-x)/x_l\right)^2$ where x_{op} is the

*Address correspondence to this author at the Faculté des Sciences de la Nature et de la Vie, Université d'Oran 1 Ahmed Ben Bella, Algeria;
E-mail: alibechlaghem@yahoo.fr

E-ISSN: 2408-977X/16 © 2016 Cosmos Scholars Publishing House

optimal doping and x_l is the width of the parabola [17, 18]. For lanthanum compound $x_{op} = 0.16$, $x_l = 0.11$ and the over-doping limit is $x_o = 0.27$, while for bismuth compound Bi2212, $x_{op} = 0.20$, $x_l = 0.15$ and the over-doping limit is $x_o = 0.35$. Both in these two compounds the onset of superconductivity occurs at $x_u = 0.05$.

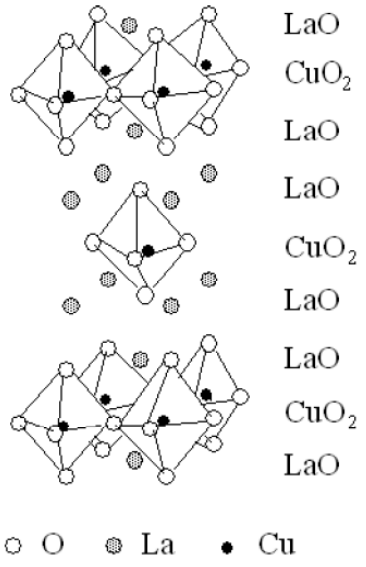

Figure 1: Atomic structure of lanthanum La_2CuO_4. The compound $La_{2-x}Sr_xCuO_4$ is doped by substitution of Sr on La sites.

These compounds differ from the conventional superconductors in various ways. They have CuO_2 planes playing a fundamental role both in the normal and superconducting states. In absence of doping these planes have strong antiferromagnetic correlation and the insulating antiferromagnetic state is converted into a metallic paramagnetic one with doping.

The atomic structure of these compounds has a very particular situation related the CuO_2 planes. For $La_{2-x}Sr_xCuO_4$ there is one CuO_2 plane per unit cell, while for the yttrium compound $YBa_2Cu_3O_{6+x}$ and Bi-2212 compound, there are two planes par unit cell. For Bi-2223 compound there are three planes per unit cell. Between these planes, inside the unit cell, there are other planes. The atomic structure of La_2CuO_4 is illustrated in Figure **1**. The CuO_2 planes are separated by square planar LaO sheets that include the apical O atoms of the octahedra.

The electron-doped superconductors have similar structures with displacements of the apical O atoms to other positions [19].

For the yttrium compound, there are two CuO_2 planes per unit cell. The yttrium plane is between the two CuO_2 planes with also BaO planes above and the CuO chains. The atomic structure of $YBa_2Cu_3O_{6+x}$, ($0 \le x \le 1$) is shown in Figure **2**.

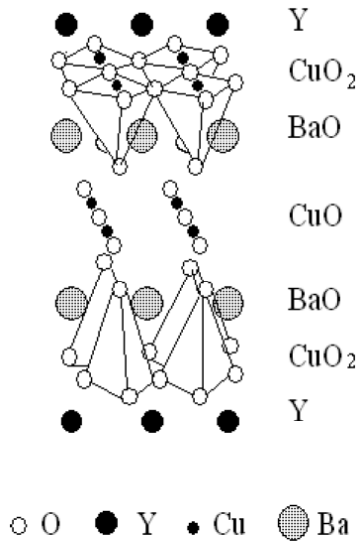

Figure 2: Atomic structure of yttrium compound $YBa_2Cu_3O_7$.

For the Bi, Tl and Hg cuprates, the different structures are often distinguished by a four-number label: m, 2, $n-1$ and n, *i.e* $(\mathrm{m}2(n-1)n, n = 2,3)$. The first number is the number of insulating layers between conducting planes, m; the second, always two, is the number of capping layers on a conducting planes, the forth is number of CuO_2 planes in a block, n; the third is the number of separating layers between CuO_2 planes in a block, $n-1$. For example Bi-2223 *i.e.* $BiSr_2Ca_2Cu_3O_{10}$ have two layers BiO, two capping layers consisting of Sr and apical oxygens, two layers of Ca separating three CuO_2 planes, the central one of which is without apical O atoms [19].

The superconducting transition temperature T_c is found to increase when the number of the CuO_2 planes per unit cell increases from $n = 1$ to 3. For example, the superconducting transition temperature T_c is 86 K and 110 K, for Bi-2212 and Bi-2223 respectively, and T_c is about 100 K and 125 K for Tl-2212, and Tl-2223 respectively. Values of maximum T_c are determined to be $T_c^{\max} = 97$ K, 123 K and 135 K, respectively, for optimally doped Hg-1201, Hg-1212 and Hg-1223.

This atomic structure of these compounds is very anisotropic, from which also follow electronic anisotropies:

- the electrical resistivity is very small in the ab

plane (CuO_2 plane) compared to the c direction [20]. For example, the electrical resistivity ratio ρ_c / ρ_{ab} is of order of 30 for yttrium compound Y-123 [21, 22], and of order of 200 - 300 for lanthanum compound $La_{2-x}Sr_xCuO_4$ [22, 23]. This ratio can vary between 30 in optimally doped $YBa_2Cu_3O_{6+x}$ to over 10^6 in $Bi_2Sr_2CuO_6$ [20-26]. The values of electrical resistivity for some cuprate superconductors are summarized in Table **1**.

Table 1: The in-Plane Resistivity $\rho_{ab}(T = 300K)$ and $\rho_c / \rho_{ab}(T = T_c)$ Values for some Cuprates at Optimal Doping [20]

Compound	$\rho_{ab}(T = 300K)$ (μΩm)	$\rho_c / \rho_{ab}(T = T_c)$
$La_{1.83}Sr_{0.17}CuO_4$	420	300
$YBa_2Cu_3O_{6.95}$	290	30
$Bi_2Sr_{1.61}La_{0.39}CuO_6$	500	$>10^6$
$Bi_2Sr_2CaCu_2O_{8+\delta}$	280	10^5
$Tl_2Ba_2CuO_6$	450	2000

- the Hall constant R_H change the sign in c or ab direction indicating the holes are in the ab planes while the electrons are in the c direction.
- the superconducting gap ratio $R = 2\Delta(0)/k_BT_c$ is large in the ab plane compared to the c direction. This anisotropy is confirmed by experimental results [28]. For yttrium compound Y-123, $R_{ab} = 5.9$ and $R_c = 3.6$, while for bismuth compounds Bi-2212 and Bi-2223, $R_c = 10$ and $R_c = 6$. This ratio has the magnitude ≈ 3.53 for the conventional superconductors, but it is much larger being $\approx$5- 13 for the hole-doped superconductors [28-37]. For the electron-doped superconductors this ratio is in the range ≈ 3.53 – 5 [37-43]. The experimental values of the superconducting gap ratio for hole-doped and electron-doped superconductors are summarized in Tables **2** and **3**, respectively. The large value of this parameter remains an open question.
- the coherence length ξ is large in the ab plane compared to c direction, for example, for the yttrium compound, the coherence length is of

Table 2: Experimental Values of the Gap Energy for Different Hole-Doped Superconductors at Optimal Doping

Compound	T_c (K)	$\Delta(0)$ (meV)	R	References
$La_{2-x}Sr_xCuO_4$	33 39	12.5 ± 0.5 17.5 ± 1.5	8.9 ± 0.2 10.3 ± 0.9	27 36
$YBa_2Cu_3O_{6+x}$	89	39.5 ± 1.5	10.6	29
$Bi_2Sr_2CaCu_2O_{8+x}$	86 92 91	41± 4 36 ± 2 32 ± 3	11 ± 1.0 9.0 ± 0.5 8.1 ± 0.8	31 31 34
$Bi_2Sr_2Ca_2Cu_3O_{10+x}$	110 110	48 ± 5 43 ± 5	10 ± 1.0 9.1 ± 1.0	28 35
$Tl_2Ba_2CuO_{6+x}$	92.5 90	43 ± 4 37	10.7 ± 1.0 9.5	29 29
$HgBa_2CuO_{6+x}$	96 97	44 ± 4 33	10.6 ±1.0 7.9	29 30
$HgBa_2CaCu_2O_{8+x}$	123	50	9.5	30
$HgBa_2Ca_2CuO_{8+x}$	130 135	60 75	10.6 13	29 30

Table 3: Experimental Values of the Gap Energy for Different Electron-Doped Superconductors at Optimal Doping

Compound	T_c (K)	$\Delta(0)$ (meV)	R	References
$Nd_{2-x}Ce_xCuO_{4-\delta}$	22	5.0 ±1.0	5.2 ± 1.1	38
$Pr_{2-x}Ce_xCuO_{4-\delta}$	19	3.3 ± 0.3	4.0 ± 0.4	39
$Pr_{1-x}LaCe_xCuO_{4-\delta}$	26 25 24	2.5 ± 0.2 3.6 ± 0.2 7.2 ± 1.2	2.2 ± 0.2 3.5 ± 0.2 6.9 ± 1.2	40 41 42

order of 15 Å in ab plane and is about 1-3 Å in c-direction. Short in-plane coherence length ξ_{ab} have been obtained for cuprate superconductors: 16 Å for $YBa_2Cu_3O_{6+x}$ [44, 45, 46], 13.6 Å for Tl-2223 [44, 47], 9.7 Å for Bi-2223 and 9 ± 1 Å for Bi-2212 [44, 48].

- the penetration depth λ is small in the ab plane compared to the c direction and the ratio λ_c / λ_{ab} is of order of 3 -10 [14]. The anisotropy of the penetration depth implies anisotropy of the effective mass: $m_c^* / m_{ab}^* \approx 25$. (Note that the symbol λ is also used for the coupling constant in temperature and gap dependences).
- the critical current j_c is large in ab plane compared to the c-direction [16]. Higher values up to j_c =10^7 A cm^{-2} have been obtained for currents parallel to the ab planes while much lower values of j_c occur along the c-direction.

The small value of the electrical resistivity in the ab planes indicates clearly that the good conductivity occurs essentially in CuO_2 planes while the other intermediate planes can be less metallic or even insulating. These CuO_2 planes are responsible of antiferromagnetism and superconductivity in these compounds.

These compounds are characterized by a small isotope coefficient α: in general this coefficient is greater than zero but it is significantly smaller than the BCS value $\alpha = 0.5$ [49-56]. For instance the isotope coefficient $\alpha \approx 0.06 - 0.09$ in $La_{1.85}Sr_{0.15}CuO_4$ with $T_c^{\max} \approx 38$ K; $\alpha \approx 0.02 - 0.03$ in $YBa_2Cu_3O_7$ with $T_c^{\max} \approx 92$ K; α ≈ 0.03 – 0.05 in $Ba_2Sr_2CaCu_2O_8$ with $T_c^{\max} \approx 86$ K; $\alpha \approx 0.03$ and even negative (α = - 0.013) in $Ba_2Sr_2Ca_2Cu_3O_{10}$ with $T_c^{\max} \approx 110$ K [55]. The deviation of α from the BCS value remains an open question.

This review is organized as follows: Section 2 describes the normal state transport properties of cuprate superconductors. Section 3 is devoted to the magnetic properties of these compounds. In section 4, we describe their two characteristic lengths: the penetration depth and the coherence length. Section 5 describes their electronic structure. In this section the density of states, charges density waves (CDWs) and spin density waves (SDWs) are discussed. In section 6, we give a brief description of the electron-phonon interaction. In section 7, we discuss the Jahn-Teller effect and the van Hove singularity. In section 8, basic ideas and assumptions of our theoretical approach are presented. In this approach, we consider the attractive interaction is due to the phonons at low temperature, but at high temperature it is related to the magnetic excitations. The coherence length, the superconducting gap ratio and the isotope coefficient are evaluated in the van Hove scenario and discussed in more detail.

2. NORMAL STATE TRANSPORT PROPERTIES

For the hole-doped cuprates, one finds on average of resistivity around 200 μΩcm [57], although for an electron-doped $Nd_{2-x}Ce_xCuO_4$ single crystal the 300 K resistivity was 600 μΩcm [58]. The in-plane resistivity $\rho_{ab}(T)$ of hole-doped cuprates (p-type) HTC varies with doping [20, 59]. The optimally doped cuprates are characterized by a T-linear resistivity that survives at $T > T_c$. This T-linear resistivity is a universal feature at optimal doping. In the under-doped cuprates, $\rho_{ab}(T)$ varies approximately linearly with temperature at high temperature T, but as the temperature is lowered, the resistivity deviates downward from linearity. In the over-doping regime, the resistivity contains a significant supralinear contribution. The electrical resistivity $\rho_{ab}(T)$ can be modeled by a three–component polynomial fit: $\rho_{ab}(T) = \rho_0 + aT + bT^2$. The observation of T^2 resistivity in $La_{1.7}Sr_{0.3}CuO_4$, coupled with Matthiessen's rule scaling, implies that the role of the electron-phonon scattering remains negligible right out to the heavily OD side of the phase diagram [20].

The resistivity in the c direction ρ_c varies with doping. In $La_{2-x}Sr_xCuO_4$, $\rho_c(T)$ changes from metallic on the over-doping side to nonmetallic bellow x < 0.14 and for x = 0.17, $\rho_c(T)$ is constant bellow 200 K. In YBa_2CuO_{6+x}, $\rho_c(T)$ varies linearly with T showing a metallic behavior down to T_c. In the low doping regime, $\rho_c(T)$ shows insulating behavior at all T. In this compound, the onset of an insulating $\rho_c(T)$ corresponds well to the crossover temperature where $\rho_{ab}(T)$ starts do deviate to linearity [60]. The ratio ρ_c / ρ_{ab} can vary between 30 for $YBa_2Cu_3O_7$ to over 10^5 in $Bi_2Sr_2CuO_6$.

In low doping regime the high-T_c superconductors are characterized by the presence of the pseudogap $\Delta_{pg}(x)$ in the normal state excitation spectrum [20]. This pseudogap decreases with doping. The resistivity $\rho_{ab}(T)$ deviates from T-linear behavior in low doping regime, and its value decreases with doping in a manner similar to $\Delta_{pg}(x)$. It appears that exist a correlation between resistivity and the pseudogap [20].

This pseudogap is identified to the separation between the Fermi energy and the van Hove singularity $|\varepsilon_F - \varepsilon_{VHS}|$ [61]. The variation of the resistivity with temperature is related to this parameter [62] and it is found to be proportional to the temperature ($\rho(T) = \rho_0 + AT$) when $|\varepsilon_F - \varepsilon_{VHS}|$ several $k_B T_c$ [48, 62-64]. The observed T^2 resistivity in the electron doped (NCCO) [65] is also consistent since $|\varepsilon_F - \varepsilon_{VHS}|$ is $>> k_B T_c$ [63]. For high temperature T, the resistivity varies linearly with the temperature, but for low T, the variation is quadratic [65].

The reduction of the quasiparticule dispersion has been observed by angle-resolved photoemission and inverse photoemission over an energy range of $|\varepsilon_k - \varepsilon_{VHS}| \leq 0.3$ eV, beyond which the quasiparticle peaks become too broad to resolve [68, 69]. This energy range is far greater than the range of phonon energies for these compounds ($\hbar\omega \leq 0.08$ eV) [44].

The parameter $|\varepsilon_F - \varepsilon_{VHS}|$ seams related to a number of other parameters describing the properties of these news compounds.

The Hall constant R_H changes sign in the hole-doped $La_{2-x}Sr_xCuO_4$ and the electron-doped $Nd_{2-x}CexCuO_4$. The sign of the Hall constant of $Nd_{2-x}CexCuO_4$ is negative in the low doping regime, but it becomes positive as the doping level is raised. There is a symmetrical change in sign of the Hall constant both in hole doped $La_{2-x}Sr_xCuO_4$ and electron doped $Nd_{2-x}CexCuO_4$.

These two compounds are symmetrical with regard to the change in the mechanism conduction with composition. In the initial stage of doping they exhibit the characteristics of a half-filled band insulator doped with holes and electrons respectively.

The superconductivity is obtained near the crossover region of the sign. This coefficient varies markedly with doping x in hole doped cuprate superconductors. Hybridization of the Cu-3 $d_{x^2-y^2}$ and O-2 $p_{x,y}$ σ^* leads to a large Fermi surface containing $(1-x)$ electron/Cu ion centered in around the X point in the Brillouin zone. In low doping regime, the Hall constant varies as: $R_H(x) \approx 1/x$, but when the doping increases, the compound becomes metallic and the Hall constant deviates from the curve expected [20].

The highest T_c composition is x = 0.15 in both of the systems, while the crossover composition of the Hall constant is higher in $La_{2-x}Sr_xCuO_4$ (x =0.30) than in $Nd_{2-x}Ce_xCuO_4$ (x =0.16). When the concentration increases, the Hall constant decreases and deviates from the expected curve in high doping regime [13]. In over doped regime, in $La_{2-x}Sr_xCuO_4$, the magnitude of R_H change sign from positive to negative at x =0.30 [13, 70]. This crossover is consistent with experimental results which support a fundamental change in the Fermi surface topology in this compound [71].

The Hall constant $R_H(T)$ decreases with the temperature T. At optimal doping this coefficient varies as: $R_H(T) \approx 1/T$. It is believed that the large magnitude of the Hall constant R_H in low doping regime suggests a loss of carriers with decreasing temperature due to the opening to the pseudogap Δ_{pg} [20].

The van Hove singularity can be expected to play a fundamental role in any strong correlation theory of superconductivity including those in which the pairing arises from spin fluctuations. It has been shown that in quasi-two dimensional *d*-wave superconductors, van Hove singularities close to the Femi surface lead to magnetic quasiparticle excitations [72]. This suggests that the superconducting pairing is mediated by these magnetic excitations.

One of the important issues in high-temperature superconductivity is the presence of the magnetic order in the superconducting state. This order parameter is still not understood. Various approaches have been proposed to study the pseudogap [73-75].

3. MAGNETIC PROPETRIES

In the thermodynamic statistical description, the magnetic correlation length $\xi_m(x,T)$ control the site order parameter $M(r)$. This correlation length $\xi_m(x,T)$ is the distance over which the magnetization changes significantly, causing a substantial decrease of local fluctuation of $M(r)$.

For lanthanum compound the Cu moments within the CuO_2 planes are antiferromagnetically ordered. Experimentally the Cu magnetic moment is equal to $M = gS\mu_B = 0.48 \pm 15\mu_B$ (μ_B is the Bohr magneton) [76]. For yttrium compound, the value of $M = gS\mu_B \approx 0.65\mu_B$ was observed at low temperature [14]. Experimental results show that the average of the Cu magnetic moment m_{Cu} is $0.60\mu_B$ and $0.55\mu_B$ for La_2CuO_4 and $YBa_2Cu_3O_{6.10}$ respectively [77, 78]. For the electron doped superconductors Pr_2CuO_4 and Nd_2CuO_4, the Cu magnetic moment is in the range $0.40\mu_B$ - $0.46\mu_B$ [81-83].

In low doping regime, the cuprate superconductors are antiferromagnetic insulators. When the doping increases, the Neel temperature $T_N(x)$ sharply decreases from its maximum value and it is suppressed to zero at critical doping x_c (Figure **3**). The variation of the Neel temperature with concentration can be expressed as [12, 61]

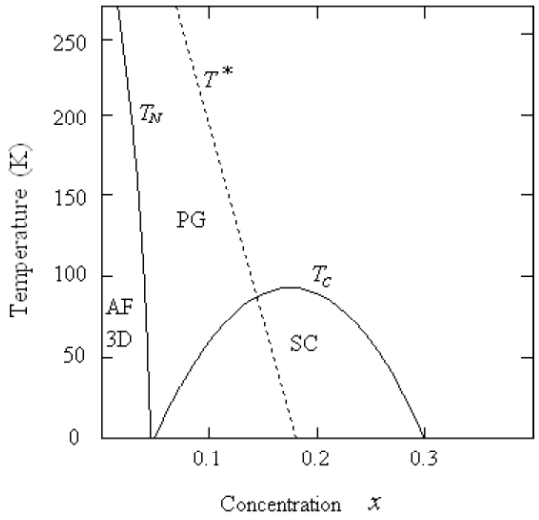

Figure 3: Phase digram of high-T_c cuprate superconducotors for $1 \le x \le 0.3$.

$$T_N(x) = T_N(0)\left(1 - \left(\frac{x}{x_c}\right)^n\right) \quad (1)$$

The concentration x varies from zero to $x_c = 0.0212$ and $n = 1.9$ for the lanthanum compound. In this range, the AF order is three-dimensional. For $0.02 \le x \le 0.08$, there is no long Neel range order and this phase is considered to be the spin glass phase. The Neel temperature $T_N(0)$, the Cu magnetic moment m_{Cu} and the superexchange J for some cuprate superconductors are summarized in Table **4**.

The superconductivity occurs only after the complete destruction of the tree-dimensional antiferromagnetic (3D AF) order. The long-range antiferromagnetic order of La_2CuO_4 is completely destroyed when 2 % of Sr is doped into the system. In $YBa_2Cu_3O_{6+x}$, the doping is coupled to tetragonal-orthorhombic transition that occurs in the vicinity of x = 0.3-0.4. This compound is an antiferromagnetic insulator in its tetragonal phase at small concentration x, and it becomes superconducting metal in its orthorhombic phase at large x.

In electron-doped superconductors such $Nd_{2-x}Ce_xCuO_4$ and $Pr_{2-x}Ce_xCuO_4$, the Neel temperature is only gradually reduced by electron-doping and the antiferromagnetic order only disappears at x = 0.14 where superconductivity appears.

The antiferromagnetic order within the CuO_2 planes is long–range with a correlation length greater than 200 Å. In the low doping regime $0.05 \le x \le 13$, there is a competition between superconductivity and spin density waves (SDWs) and when the concentration increases the SDW parameter decreases giving rise to superconductivity.

Neutron measurements reported the observation of propagating spin waves at scales larger than J [84]. The medium range magnetic correlations are still present at optimal doping and the short-range AF domains survive in high doping regime. The persistence of two-dimensional spin ordering on doping is detected by experimental results [85].

The magnetic correlation $\xi_m(x,T)$ decreases when the concentration x increases and it is about equal to the average spacing between the doped holes (Figure **4**). This fact indicates that the magnetic ordering survives in highest T_c superconducting region $x \approx 0.15$.

Table 4: Experimental Values of the Neel Temperature T_N, the Cu Magnetic Moment m_{Cu} and the Superexchange Energy J for some Cuprate Superconductors

Compound	T_N (K)	m_{Cu} (μ_B)	J (meV)	References
La_2CuO_4	325	0.60	146	77
$YBa_2Cu_3O_{6.1}$	410	0.55	106	78
$TlBa_2YCu_2O_7$	>350	0.52		79
$Ca_{0.85}Sr_{0.15}CuO_2$	537	0.51		80
Nd_2CuO_4	276	0.46	155	81
Pr_2CuO_4	248	0.40	130	81

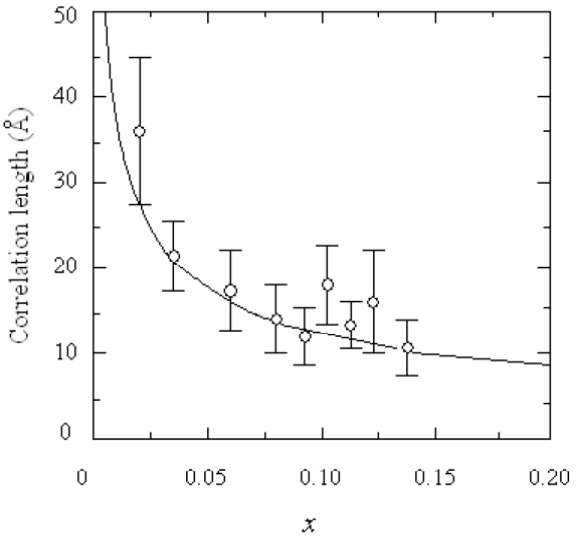

Figure 4: Variation of the magnetic correlation length ξ_m with the hole concentration x in $La_{2-x}Sr_xCuO_4$. The solid line is the relation $5.4/\sqrt{x}$ (Å) [13, 85]

In the interval 10-300 K, the magnetic correlation length has been deduced to be of order of 18 ± 6 Å for $x \approx 0.11$ for T_c = 26 K and it is about 10 Å for x = 0.20 corresponding to T_c = 30.5 K. The variation of $\xi_m(x,T)$ with concentration x can be expressed as [86]

$$\xi_m(x,T) \cong x^{-1/2} e^{0.85/2xT} \tag{2}$$

The variation $\xi_m(x,T)$ with concentration x is illustrated in Figure **5**. We remark that experimental values obtained from NQR are in good agreement with those obtained from neutron scattering.

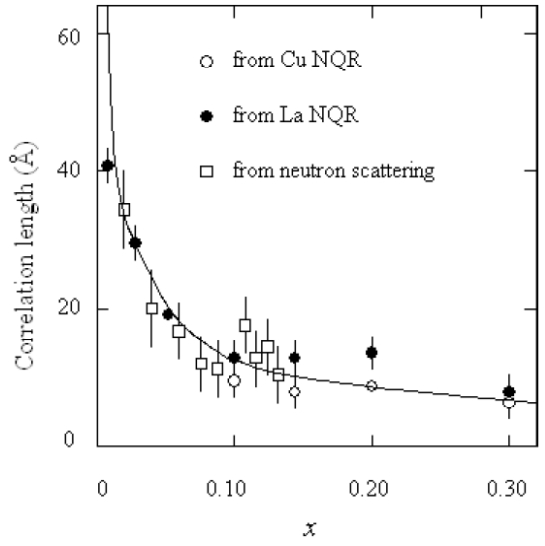

Figure 5: Variation of the magnetic correlation length ξ_m with the hole concentration x in $La_{2-x}Sr_xCuO_4$ at T = 77 K, as derived from NQR for ^{139}La and ^{63}Cu and comparison with the results obtained through the neutron scattering. The solid line is the relation given by Eq. (2) [86].

The magnetic correlation $\xi_m(x,T)$ could be fitted to the form [87]

$$\xi_m(x,T)^{-1} = \xi_m(x,0)^{-1} + \xi_m(0,T)^{-1} \tag{3}$$

where $\xi_m(x,0) = \xi_m(x)$ and $\xi_m(0,T) = \xi_m(T)$ This form is expected for phase separation if the magnetic domain have size $\xi_0(x)$. This allows an estimate domain size $\xi_0(0.02) = 200$ Å, $\xi_0(0.04) = 40$ Å. From mean field theory, the AF domain scales like $L(x) \propto x^{-n/2} \propto 1/x$.

Experimental results show strong antiferromagnetic correlations in yttrium compound $YBa_2Cu_3O_{6+x}$ [88]. The magnetic correlation decreases with x and it is about equal to lattice parameter a for x = 1. This indicates clearly that AF spin ordering survives in high-T_c. Experimental results show that the pseudogap decreases with the concentration and goes to zero at optimal doping corresponding to maximum T_c [88-89]. The first evidence came from NMR measurement [90] on two YB_2CuO_{3+x} samples, a slightly overdoped sample ($x = 0.97$) and an underdoped sample ($x = 0.64$). This pseudogag has been interpreted in terms of a spin gap, arising within a purely magnetic model of cuprates.

The lanthanum $La_{2-x}Sr_xCuO_4$ and yttrium YB_2CuO_{3+x} compounds are antiferromgnetic insulators in their tetragonal phase at small x, and become superconductors in the large x orthorhombic phase. The separation between these two singularities in the tetragonal phase is proportional to the SDW order parameter. This parameter decreases when the concentration x increases. Other experimental results [91, 92] show that there is a coexistence between the two-dimensional antifrromagntism (2D AF) and superconductivity state of the CuO_2 planes with a short magnetic correlation length which decreases with x. For lanthanum compound $La_{2-x}Sr_xCuO_4$ and 2212 bismuth compound, it has been shown that $T_c(x)$ and $T_N(x)$ disappear together when the system becomes metallic for higher x value. This suggests that 2D AF favors superconductivity because the the corresponding magnetic fluctuations can give an attractive interaction between two electrons or holes related to the exchange magnetic excitations [16]. The magnetic correlation $\xi_m(T)$ decreases with temperature T and can be expressed as $\xi_m(T) \propto \exp(C/T)$ [73].

The theoretical analysis of the correlation length give the essential following result [93-96]

$$\xi / a \propto e^{2\pi\rho_{s!}T} \tag{4}$$

where the spin stiffness ρ_s is proportional to the superexchange energy J. The experimental results are in good agreement with theory [93].

4. THE TWO CHARATERISTIC LENGTHS

There are two important microscopic lengths that characterize the magnetic properties of superconductors: the coherence length ξ and the penetration depth λ. These microscopic lengths are two of the key parameters describing the superconducting state.

In conventional superconductors, the coherence length ξ is about $\approx 10^3 - 10^4$ Å, and the penetration depth λ is about $\approx$160 – 1100 Å, but in high-T_c superconductors, ξ is in the range ($\approx$ 9 – 40 Å) and λ is about $\approx$1000-20000 Å.

All of the cuprate superconductors are type-II superconductors, with $\kappa = \lambda_L / \xi > 10$. The coherence length is anomalously small and the penetration depth λ is anomalously large.

For the superconducting oxide the anisotropy is large: $\lambda_c / \lambda_{ab} \approx 3 - 10$ and $\xi_{ab} / \xi_c \approx 5$.

4.1. The Coherence Length

The high-T_c cuprate superconductors are characterized by short coherence length ξ. Experimental results show that short coherence lengths have been obtained for some of high-T_c Cu oxide superconductors: 16 Å for $YBa_2Cu_3O_{6+x}$ [44, 45], 13.6 Å for Tl-2223 [46], 9.7 Å for Bi-2223 and 9 ± 1 Å for Bi-2212 [47, 48]. Other experimental results show that the coherence length is about 25 Å for yttrium compound [94]. For lanthanum compound $La_{2-x}Sr_xCuO_4$, if we estimate the coherence length between 20 Å and 40 Å, the ratio ξ / a is about ≈ 5 – 10 and about 2.5 – 4 for other cuprate superconductors (the lattice parameter is about *a* ≈ 4 Å). Several other exotic superconductors have nearly the same ratios ξ / a ≈ 2.5 – 3.5 [44]. These results are very smaller than the typical ratios ξ / a of 10^3 for the conventional superconductors. For comparison some ξ / a values for pure metals are: Al, 5600; In, 1.100; Sn, 760; Pb, 250; Nb, 200 [44]. We remark that these values of the coherence length are very small relative to their values in conventional superconductors. The properties of the coherence length will be discussed in more detail in section 8.

4.2. The Penetration Depth

The high-T_c cuprate superconductors are characterized by a large value of the penetration depth. This penetration depth for an isotropic superconductor is given by

$$\lambda(0) = \left(\frac{m^*}{\mu_0 n_s e^2} \right)^{1/2} \tag{5}$$

where m^* is the effective mass of carriers, μ_0 the permeability of vacuum, n_s the concentration of the superconducting state and e the electron charge. If we suppose that all electrons are superconducting at temperature T = 0 and n_s =10^{29} m^{-3}, we obtain $\lambda(0)$ = 168.55 Å for the conventional metal superconductors. But in the cuprate superconductors the value of $\lambda(0)$ is large compared to its value in the classical superconductors.

In these cuprate superconductors the supercourents flow predominantly in the CuO_2 plane giving rise to an anisotropic penetration depth. The anisotropy of λ implies anisotropy of the effective mass and the London formula given by Eq. (5) has the more general form [97-99]

$$\lambda(0) = \left(\frac{m^*_{ab,c}}{\mu_0 n_s e^2} \right)^{1/2} \propto \left(\frac{m^*_{ab,c}}{n_s} \right)^{1/2} \tag{6}$$

where m^*_{ab} (m^*_c) is the effective mass of the superconducting carriers associated with λ_{ab} (λ_c). In polycrystalline sample one measures an effective penetration depth λ_{eff} which is independent of the anisotropy ratio and is determined by λ_{ab} [97, 99]:

$$\lambda_{eff} \approx 1.23\lambda_{ab} \tag{7}$$

The values of $\lambda_{ab}(0)$ and $\lambda_c(0)$ can be deduced from the penetration depth λ_{eff} = 155 nm and the known $\lambda_c / \lambda_{ab} \approx 5$. Using Eq. (7), one obtain the values of $\lambda_{ab}(0)$ and $\lambda_c(0)$ at T = 0: $\lambda_{ab}(0)$ = 133 nm and $\lambda_c(0) \approx$500-800 nm. These results are consistent with the experimental values of the penetration depth and the anisotropy ratio of $YBa_2Cu_3O_{6+x}$ obtained with other various methods [100-105]. All these experiments

show that $\lambda_{ab}(0)$ is in the range 130- 141.5 nm and $\lambda_c(0)$ is in the range 500- 800 nm.

At higher temperatures we expect n_s to decrease and $\lambda(T)$ to increase. The temperature dependence is often well described by

$$\lambda(T) = \frac{\lambda(0)}{\left[1-\left(T/T_c\right)^4\right]^{1/2}} \quad (8)$$

where $\lambda(0)$ is the value of penetration depth at T = 0. The penetration depth increases with T and diverges as $T \to T_c$ and $n_s(T) \to 0$.

The variation of the effective penetration depth $\lambda_{eff}(T)$ with temperature for high quality sintered $YBa_2CuO_{6.97}$ sample is shown in Figure **6**. This effective penetration depth is very well described by the empirical formula given by Eq. (8). The properties of the effective penetration depth $\lambda_{eff}(T)$ and the ratio $\lambda_c/\lambda_{ab} \geq 5$ are very well analyzed by Keller in Ref. [99].

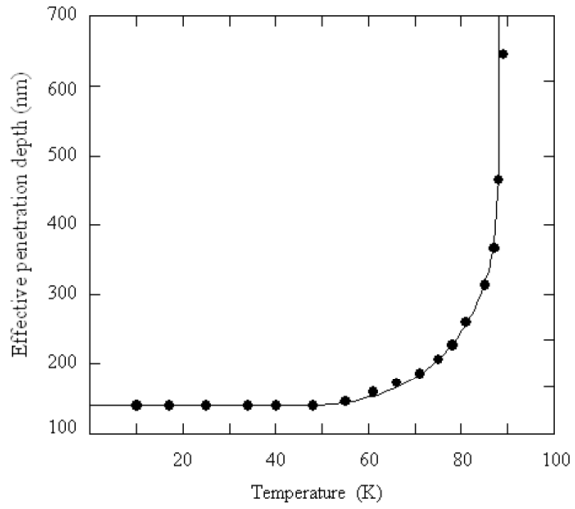

Figure 6: The variation of the penetration depth λ_{eff} with the tmeperature T for yttrium compound $YBa_2Cu_3O_{6+x}$ ($x = 0.97$, $T_c = 89.5$ K) measured in a field of 350 mT. The solid curve is a fit using the empirical expression given by Eq. (8) [99].

In tight-binding BCS type model of layered high-temperature superconductors [98], the theoretical values of $\lambda_{ab}(0)$ and $\lambda_c(0)$ are in qualitative agreement with experimental results [100-105]. The values obtained in this model [98] are in the range 940 -1878 Å for $\lambda_{ab}(0)$ and in the range 6738- 4992 Å for $\lambda_c(0)$ and the value of the effective m^*_{ab} is in range $2.70m_0$ - $10.84m_0$.

In our approach the effective mass m^* is in the range $2m_0$ - $6m_0$ [106]. Therefore we obtain the values of $\lambda_{ab}(0)$ in the range 752.56 Å – 1303.46Å for carrier concentration $\approx 10^{22}$ cm^{-1}. For $m^* = 2m_0$, the value of $\lambda_{ab}(0)$ is in the range 752.55Å – 2380 Å when the carriers concentration is in the range $10^{21} - 10^{22}$ cm^{-1}. These values are in good agreement with experimental results [99-105].

5. ELECTRONIC STRUCTURES

5.1. Basic Cristal Structure

The high-T_c cuprate superconductors have CuO_2 planes playing a fundamental role both in the normal and superconducting states. Between the CuO_2 planes there are other layers which serve as charge reservoirs to these planes. For the lanthanum compound La_2CuO_4, the valence of Cu is $2+$ corresponding to $3d^9$ electronic configuration. Since the Cu^{2+} is surrounded by six oxygen atoms, two of them lying above or below the plane, and the four others inside the plane, the crystal field splits the otherwise degenerate five d-orbitales. The four lower energy orbitals including d_{xy}, d_{xz}, d_{yz} and $d_{3z^2-r^2}$ are fully occupied, while the highest energy $d_{x^2-y^2}$ is half filled. The covalent bond is obtained from the filling of electrons in the bonding orbital of $Cu_{3d(x^2-y^2)} - O_{2p}$ and the half-filling of the anti-bonding orbital σ^*_{dp} (Figure **7**)

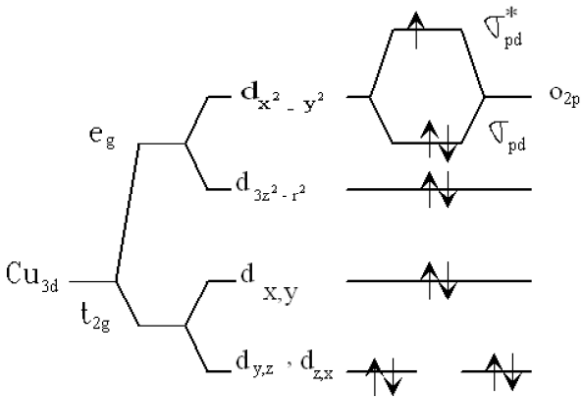

Figure 7: Illusration of the formation of the bonding and antibonding in CuO_2 planes. Splitting of $3d$ orbital energy in the square coordinated environment. The atomic Cu $3d$ level is split into eg and t_{2g} states. There is a further splitting into x^2-y^2, $3z^2-r^2$, xy and yz, zx. There is hybridization of the Cu states, particularly x^2-y^2 with the O $2p$ states thus forming a half-filled two-dimensional Cu $3d_{x^2-y^2}$ – O $2p_{x,y}$ antibonding band.

[3, 13, 107]. The Bloch wave function can be written as the following linear combination [3]

$$\psi_k(k,r)=\frac{1}{\sqrt{N}}\sum_R e^{kR}\left[A_k d_{x^2-y^2}(r-R)+B_k p_x(r-R\frac{a_1}{2})+B_k p_x(r-R\frac{a_2}{2})\right] \quad (9)$$

The band dispersion is given by

$$\varepsilon(k)=\begin{cases}\dfrac{(E_p+E_d)}{2}\pm\dfrac{1}{2}\sqrt{\left(E_d-E_p\right)^2+8\gamma^2\left(2-\cos k_x a-\cos k_y a\right)}\\ E_p\end{cases} \quad (10)$$

where E_p and E_d denote the energy of the p orbitals of oxygen and of the d orbitals of copper respectively and γ is the transfer integral between $d_{x^2-y^2}$ and p_x or p_y. The logarithmic singularities of $n(\varepsilon)$ are obtained at the energies

$$E_s^{\pm}=\frac{1}{2}\left(E_d+E_p\right)\pm\frac{1}{2}\sqrt{\left(E_d-E_p\right)^2+16\gamma^2} \quad (11)$$

There are four van Hove singularity points at $k=(\pm\pi/a,\ 0)$ and $k=(0,\pm\pi/a)$. When the Fermi energy is low, the Fermi surface is circular. As the Fermi energy is raised, the Fermi surface is distorted and becomes a square at the half-filled position. When the Fermi energy $\varepsilon_F=E_s$, the Fermi surface is a square and perfect nesting can be occurred.

5.2. Form of the Density of States

When the ratio $t=\gamma^2/(E_d-E_p)\ll 1$, Eq. (10) can be written in its simple form

$$\varepsilon_k=4t-2t\left(\cos k_x a+\cos k_y a\right)=\varepsilon_E-2t\left(\cos k_x a+\cos k_y a\right) \quad (12)$$

where t appears as an effective transfer integral between two atoms of copper. The Fermi surface is a perfect square. This leads to instability against formation of a spin or charge density wave, in addition to the Cooper pairing which is independent of the Fermi surface topology. The presence of saddle points of $\varepsilon(k)$ gives rise to a logarithmic van Hove singularity of the density of states which is given by [3]

$$n(\varepsilon)=\frac{1}{2\pi^2 t}\ln\frac{16t}{\left|\varepsilon-\varepsilon_F\right|} \quad (13)$$

Another work [108] shows that the density of states $n(\varepsilon)$ derived from a tight-binding model on a two dimensional square lattice contain a logarithmic term plus a constant one $n(\varepsilon)=n_1\ln\left(D/|\varepsilon|\right)+n_0$, where $n_1=1/2\pi^2 t$, $D=4t$ and $n_0=\left(1/2\pi^2 t\right)\ln 4$. The density of states can be expressed as

$$n(\varepsilon)=\frac{1}{2\pi^2 t}\ln\frac{4t}{\left|\varepsilon-\varepsilon_F\right|}+\frac{1}{2\pi^2 t}\ln 4 \quad (14)$$

The Fermi surface is a perfect square and near the singularity, the density of states is $n(\varepsilon)=(1/2D)\ln\left(D/|\varepsilon|\right)$ where $D=\pi^2 t$ [109]. Near the band edge the two-dimensional electronic spectrum is developed as $\varepsilon(\mathbf{k})-\varepsilon_F=t\left(\left(k_x a\right)^2+\left(k_y a\right)^2\right)$ which leads to a constant of the density of states $n_0=1/4\pi t$.

In the free electron model, the two-dimensional electronic spectrum is given by

$$\varepsilon(k)=\varepsilon_F+\frac{\hbar^2}{2m^*}k_x k_y \quad (15)$$

From this expression, we have obtained the same formula of the density of states $n(\varepsilon)$ [106]

$$n(\varepsilon)=n_s(\varepsilon)+n_0=\frac{2m^*a^2}{\pi^2\hbar^2}\ln\frac{\pi^2\hbar^2}{4m^*a^2\left|\varepsilon-\varepsilon_F\right|}+\frac{m^*a^2}{2\pi\hbar^2} \quad (16)$$

We can write the general density of states $n(\varepsilon)$ as

$$n(\varepsilon)=n_1\ln\frac{D}{\left|\varepsilon-\varepsilon_F\right|}+n_0 \quad (17)$$

With this form of the density of states, we evaluate the major parameters for the cuprate superconductors.

5.3. Fermi Surface Instability, SDW and CDW

The possibility of the Fermi surface instability was considered because of the 2D square shape of the Fermi surface expected for the half-filled σ_{dp}^* [13]. When the Fermi energy is low, the band gives a free electron like circular Fermi surface. As the Fermi energy ε_F is raised, the Fermi surface is distorted from a circle and becomes a square at half-filled position.

The lattice can be distorted because of the Coulomb interaction between lattice and charge. In these compounds, there is a competition between electron-electron interaction and electron-phonon interaction when the doping increases. The possibility of spin density waves and charge density waves are formed. Conventional superconductivity and charge density waves (CDWs) are produced by strong electron-

phonon coupling. Spin density waves (SDWs) are produced by strong electron-electron repulsion which tends to destroy superconductivity. The large electron-electron interaction V_C favors the formation of SDW and tends to suppress the superconductivity. On the other side, large electron-phonon interaction V_p favors superconductivity and destroys SDW. For small values of both parameters both possible broken symmetries destroy each other giving rise to a paramagnetic phase. For large values of both parameters V_C and V_p, both superconductivity and SDW coexist in a large proportion of the phase space [110]. In general there is coexistence between density spin density waves or charge density waves (SDWs or CDWs) and superconductivity in high-T_c superconductors. We mention that experimental results show that there is coexistence between charge or spin density waves (CDWs or SDWs) and superconductivity in $La_{2-x}Sr_xCuO_4$ and $YBa_2Cu_3O_{6+x}$ [111-113]. The CDW is strongest with the longest in-plane correlation length near 1/8 doping. On entering the superconducting state the CDW is suppressed [111]. In low doping situation the long range antiferromagnetic order is destroyed to give rise to SDW state accompanied by a CDW state in the system due to doping. For suitable doping the superconductivity appears in the system. The significance of the various forms of CDW and SDW is still not understood. Their detection, characterization and relationship with superconductivity remain an open problems.

The model for the density of states of a two-dimensional system is unstable at half-filling in view of nesting effect [114]. We believe that instability is due to the magnetic excitations or thermodynamic fluctuations. The role of the singularity in the mechanism of high-T_c superconductivity and the stability of the system are not yet established but we want to stress that this model has already explained a certain number of experimental facts, *i.e* high T_c [3], small isotope effect [108, 110], linear resistivity and thermopower [67], and other properties. We focus on the role of the van Hove singularity that will be present in stable situations.

5.4. Evolution of the Electronic Structure from Insulator to Superconductor

The electronic structure of the high cuprate superconductors evolutes with doping. In absence of doping the planes CO_2 have strong antiferromagnetic correlation ant the insulating antiferromagnetic state is converted into a metallic paramagnetic one with doping.

In undoped cuprates, the strong Coulomb interaction V_C on the same Cu site makes them antiferromagnetic insulators with energy gap of 2 eV. In the normal state, the Coulomb interaction is very large and estimated to be 6 to 8 eV and the valence band is about 6 to 7 eV wide [115]. The electron-electron interaction produces spin density waves (SDWs).

The band predicts a large Fermi surface which corresponds to high carriers density that varies with doping. The doping with a very small number of holes would lower the Fermi energy through the band and produce a Fermi surface with pockets centered at $(\pi/2a, \pi/2a)$. For p-type doping an important difference in band shape between the insulator and the metal is the existence of the saddle points close to the Fermi level near $(\pi/a, 0)$ that are missing in the insulator. The lowest energy band in the insulator and the band that crosses ε_F in the hole doped metals are very similar. The band is separated from the valence band in the same way, it has similar dispersion, and it has similar intensity modulation as a function of energy.

In the metallic phase, the electronic structure is affected by short-range antiferromagnetic spin fluctuations [115]

6. ELECTRON-PHONON COUPLING

It is well known in conventional superconductors, electron-phonon coupling is responsible for Cooper pairs. In metals, the kinetic energy or the Fermi energy ε_F is of order of 1-10 eV [116, 117] and the phonon energy is much smaller ($\approx$ 1-100 meV) [107]. In the insulator, the kinetic energy is much smaller than the phonon energy and the carrier can be dressed by a thick phonon cloud and its effective mass can be very large. In general when the kinetic energy of particles is less than the phonon energy, the dressing of the phonon cloud could be large and the electron-phonon coupling enters into polaron regime.

The electron-phonon coupling could play a fundamental role in high-T_c superconductors. This interaction is characterized in two categories: a) weak coupling, b) strong coupling and polaron regime. The weak electron-phonon coupling is useful in accounting for many observations. For example, in the cuprate superconductors, the Fermi energy is of order 0.1 – 1 eV and the phonon frequencies are in the range 335-640 cm^{-1}[118]. However there are experimental indications that defy weak electron-phonon coupling. Weak electron-phonon coupling or strong electron-phonon coupling remains an open question.

A new interpretation of the role of electron–phonon interactions in electron pairing in superconductivity is recently suggested [119] by comparison with the

conventional Bardeen–Cooper–Schrieffer (BCS) theory. In this interpretation, vibronic stabilization for independent one-electron systems as well as for two-electrons systems can be explained by one-electron theory. The vibronic and Jahn–Teller stabilization energy in the opened-shell electronic states can be considered to originate from the second-order processes in the vibronic and electron–phonon interactions between two electronic states of independent one electron, in view of one-electron theory.

7. JAHN-TELLER EFFECT

The Jahn-Teller (JT) effect was initially developed for molecules and applied to isolated impurities in solids. The Jahn-Teller theorem states that whenever a molecule has an electronic degeneracy, there is a molecule distortion which splits the degeneracy. This degeneracy in a molecule is instable [61].

The molecule with an electronic degeneracy can lower its energy by distorting spontaneously. If the energy barrier is small, the molecule can tunnel between several equivalent distortions, giving rise to the dynamic Jahn-Teller effect. In a crystalline solid, the electronic degeneracy is associated with the two Fermi surface points.

The coupling can always be related to the Jahn-Teller effect of the Cu^{2+} cation. It has been shown that the Jahn-Teller effect of the Cu^{2+} cation brings about an attractive pairing interaction between the hybridized $3d^9$ electrons states [5].

The Cu^{2+} is a typical Jahn-Teller cation which distorts the copper oxygen bondings and lowers the electronic energy level, yielding to so called Jahn-Teller polaron [5]. This concept led to the discovery of high temperature superconductivity in hole doped La_2CuO_4 [120].

In the lanthanum compound $La_2Sr_xCuO_4$, the distortion of CuO_6 octahedra is a typical JT effect. The displacement of the oxygen anions leads to the elongation Cu-apical O distance. This elongation is the JT distortion which splits the d hole degeneracy.

The Jahn-Teller effect has been already considered as responsible for high critical temperature in high-T_c superconductors [4, 5, 7-9, 121-126].

The isotope effect observed in high-T_c superconductors is probably due to the Jahn-Teller effect. Based on this effect, Apostol has obtained high critical temperature T_c, small isotope effect α and relatively large superconducting gap ratio $R = 2\Delta(0)/k_B T_c$ in lanthanum and yttrium compounds. His theoretical results [123] for T_c and α are in good agreement with experimental results. There is a function of x a tetragonal-orthorhombic transition with a =3.83 Å and b = 3.88 Å; along the direction perpendicular to CuO_2 plans, one can define the c axis whose unit cell periodicity is of order of 11.7 Å [16]. This structural transition from a tetragonal to orthorhombic phase has been already considered important in high-T_c superconductors. When the Fermi level ε_F coincides with singularity, a band Jahn-Teller effect is expected, which leads to structural phase transition from the tetragonal phase to an orthorhombic one [3].

The unique van Hove singularity in tetragonal phase is splitted into two singularities with the Fermi level lying between them, in a region where the density of states is low [3, 15]. The electronic degeneracy is associated with these two singularities. Any structural distortion which splits this degeneracy is called a SVH-JT effect [61]. This effect is pointed out by Friedel [127] and applied to cuprates by Markiewicz [128-130].

The VHS-JT model predicts a competition between structural instability and superconductivity.

8. THEORETICAL APPROACH

8.1. Basic Hypothesis and Assumption

The high-T_c superconductors have quazi-2D structure. All their properties show that the good conductivity occurs in the CuO_2 planes. These planes are antiferromagnitic insulators in low doping regime. This nearly 2D-structure leads naturally to van Hove singularities in the density of states. We consider a two-dimensional system to describe and evaluate the major parameters of these compounds. To do this, we consider

- perfect periodicity of the crystal,
- the singularity is present in a stable situations and the Fermi energy lies close to the van Hove singularity,
- at low temperature, the pairing is due essentially to the phonons.
- at high temperature, the pairing is due essentially to the magnetic excitations.

8.2. Calculation of T_c

The general equation giving the gap Δ at temperature T in BCS theory is given by [131]

$$\Delta(T) = -\frac{1}{2}\sum V_{k,k'} \frac{\Delta_{k'}(T)}{\sqrt{\varepsilon_{k'}^2 + \Delta_{k'}^2(T)}} \tanh\left(\frac{\sqrt{\varepsilon_{k'}^2 + \Delta_{k'}^2(T)}}{2k_B T}\right) \tag{18}$$

Near T_c , the gap energy Δ goes to zero and Eq. (18) becomes

$$1 = -\frac{1}{2}\sum_{k'} \frac{V_{k,k'}}{\varepsilon_{k'}} \tanh\left(\frac{\varepsilon_{k'}}{2k_B T_c}\right) \tag{19}$$

The improvement here is to consider two types of interactions. The first one is related to the phonons which is described in BCS theory by a constant attractive matrix element $-V_p$ ($V_p > 0$) and the second due to the magnetic excitations $-V_m$ ($V_m > 0$) which is considered constant from $-W/2$ to $+W/2$ where W is bandwidth.

8.2.1. Expression of T_c at Low Temperature

Based on our hypothesis, at low temperature, the attractive interaction is due to the phonons V_p which is constant between $-k_B\theta_D$ and $k_B\theta_D$. Introducing Eq. (17) in Eq. (19) we obtain the following expression of T_c at low temperature

$$k_B T_c = 1.13D \exp\left(\frac{n_0}{n_1} - \left[\frac{2}{\lambda_p} + \left(\frac{n_0}{n_1} + \ln\frac{D}{k_B\theta_D}\right)^2 - p\right]^{\frac{1}{2}}\right) \tag{20}$$

If we neglect the singularity ($n_1 \to 0$), we obtain the BCS formula

8.2.2. Expression of T_c at High Temperature

Based on our hypothesis, the attractive interaction is due essentially to the magnetic excitations $-V_m$ ($V_m > 0$). This interaction is considered constant from $-W/2$ to $+W/2$, This interaction is very well described in Ref. 6 and has the form

$$V_m = \frac{K^2}{J} \tag{21}$$

where K is the Kondo-type exchange interaction between spins responsible for conduction and copper spins Cu($K = J_{pd}$) and J ($J = J_{dd}$) is the exchange interaction between two Cu spins. This interaction has the approximate expression [6]

$$J \cong j_0 \exp\left(-\frac{1}{2d^2}\frac{\hbar}{2M\omega_0}\right) \tag{22}$$

where d is a characteristic length for the overlap of wave functions and M is the mass of oxygen or copper ion and $\hbar\omega_0$ is the $\mathrm{Cu-O}$ vibrational energy. Introducing Eq. (17) in Eq. (19) we obtain the following expression of T_c at high temperature

$$k_B T_c = 1.13D \exp\left(\frac{n_0}{n_1} - \left[\frac{2}{\lambda_m} + \left(\frac{n_0}{n_1}\right)^2 - p\right]^{\frac{1}{2}}\right) \tag{23}$$

If we neglect the singularity ($n_1 \to 0$) and we take $D = J$, we obtain the Kurihara formula [6]

8.2.3. General Expression of T_c

Introducing Eq. (17) in Eq. (19) and taking into account the two interactions, we obtain

$$1 = (V_p + V_m)\int_0^{k_B\theta_D} \frac{\tanh(\varepsilon/2k_B T_c)}{\varepsilon}\left(n_0 + n_1 \ln\frac{D}{\varepsilon}\right)d\varepsilon$$

$$+V_m \int_{k_B\theta_D}^{W/2} \frac{\tanh(\varepsilon/2k_B\theta_D)}{\varepsilon}\left(n_0 + n_1 \ln\frac{D}{\varepsilon}\right)d\varepsilon \tag{24}$$

Analytical and numerical calculations give [132]

$$k_B T_c = 1.13D \exp\left\{\frac{n_0}{n_1} - [A - B]^{\frac{1}{2}}\right\} \tag{25}$$

where

$$A = \frac{2}{(V_p + V_m)n_1} + \left(\frac{n_0}{n_1} + \ln\frac{D}{k_B\theta_D}\right)^2 - 1.32 \tag{26}$$

and

$$B = \frac{V_m}{(V_p + V_m)n_1}\left[2\frac{n_0}{n_1}\ln\frac{D}{k_B\theta_D} + \left(\ln\frac{D}{k_B\theta_D}\right)^2\right] \tag{27}$$

It is interesting to note that Eq. (25) does not provide any upper limit. In fact this equation is also applicable to low as well as high-T_c superconductors. For the conventional superconductors, there is neither singularity ($n_1 \to 0$) nor magnetic excitations and $D = k_B\theta_D$, Eq. (25) leads to the BCS formula.

For the cuprates, the singularity and the magnetic excitations are not negligeable. In this case some cases are possible:

(1) for $V_m = 0$ we find the expression of T_c obtained from the gap energy equation [133]. In this case, if we replace the coupling constant $\lambda_p = n_1 V_p$ by $\lambda_p - \mu^*$ where the pseuopotential μ^* given by [134]

$$\mu^* = \frac{n_1 V_c}{1 + n_1 V_c \left[\frac{1}{2} \left(\ln \frac{D}{k_B \theta_D} \right)^2 + \frac{n_0}{n_1} \ln \frac{D}{k_B \theta_D} \right]} \quad (28)$$

we have the expression obtained by Force-Bok. In this case, the Coulomb interaction V_C has a strong effect in reducing T_c but does not suppress superconductivity.

(2) for $V_m = 0$ and $n_1 = 0$, three cases are possible, a)when $D = \varepsilon_F$, this leads to an exact result than obtained by Tsuei *et al* [135], b) when $D = 16t$, t being intersite transfer integral, we have the expression obtained by Germain and Labbé [15], c) when $D = 21.17796t$, we obtain the expression obtained by Szczesniak *et al* [136]. In these cases, the Debye energy enhances the superconducting transition temperature. For example T_c increases from 10.22 K to 19.30 when the Debye energy varies from 0.025 eV to 0.065 eV.

(3) for $V_p = 0$, we find the expression of T_c obtained in a previous work [137]. In this case, T_c is independent on the Debye energy and the isotope coefficient $\alpha = 0$.

(4) for $V_p = 0$, $n_1 = 0$ and $D = J$, we obtain the Kurihara formula [6].

Equation (25) is a general expression describing the high-T_c superconductors. At low temperature, the pairing is due essentially to the phonons and the superconductivity in the electron-doped cuprates is very well described by Eq. (20). With the expression (20), we obtain easily T_c = 22 K for $Nd_{2-x}Ce_xCuO_4$ (NCCO), T_c =19 K for $Pr_{2-x}CuO_4$ (PCCO) and T_c = 24-26 K for $Pr_{1-x}LaCe_xCuO_4$ (PLCCO).

At high temperature the superconductivity in hole-doped cuprates is very well described by equation (23). With this expression, we obtain easily T_c = 96 K, 123 K and 135 K for optimally doped Hg-1201, Hg-1212, and Hg-1223. In the intermediate temperatures, the superconductivity is very well described by Eq. (25)

8.3. Properties of the Two-Gap Parameters

The total gap $\Delta(T)$ is constant and can be expressed as

$$\Delta(T) = \sqrt{\Delta_{sg}^2(T) + \Delta_{pg}^2(T)} \quad (29)$$

where $\Delta_{sg}(T)$ is the superconducting gap (SC) and $\Delta_{pg}(T)$ is the pseudogap (PG). At low temperature the total gap is a pure SC, but at high temperature it is a pure pseudogap, and at intermediate temperature the gap has two contributions, one form the superconducting gap and the other form the pseudogap. Just as there are two gap parameters, there are two temperature scales: the pseudogap temperature T^* marking the appearance of the pseudogap and T_c which marks the appearance of the superconductivity. The superconducting gap vanishes at T_c, while the pseudogap exists both above and below T_c. This behavior is illustrated in Figure **8**. At $T = 0$, the gap is equal to $\Delta(0) = \Delta_{sg}(0)$ and at $T = T_c$ the gap is equal to $\Delta(T_c) = \Delta_{pg}(T_c)$. Above $T = T_c$ the pseudogap decreases and is suppressed to zero at $T = T^*$. At temperatures $T_c < T < T^*$ the total gap is a pure pseudogap: $\Delta(T) = \Delta_{pg}(T)$. When the concentration decreases, the pseudogap increases while the superconducting gap decreases. The SG and the pseudogap PG are anisotropic: they have maximum values along 100 and 010 directions and have minimum values along 110 direction. Many studies have shown that Δ_{sg} has *d*-wave symmetry and Δ_{pg} has a similar anisotropy where $\Delta_{sg}(\mathbf{k})$ can be expressed as $\Delta_{sg}(\mathbf{k}) = \Delta_{sg} \cos(2\theta)$ and $\Delta_{pg}(\mathbf{k}) = \Delta_{pg} |\cos(2\theta)|$ [138 – 141]. It believed that the

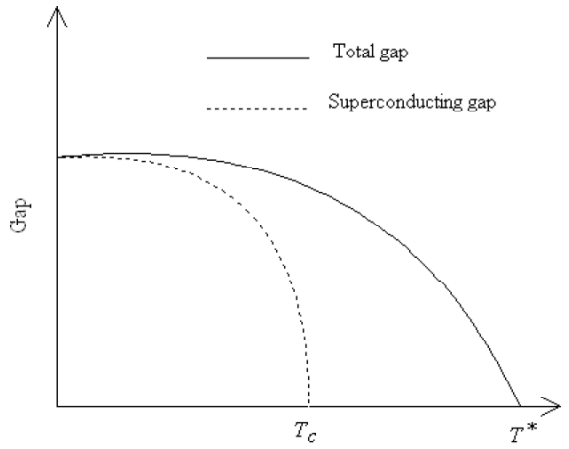

Figure 8: Variation of the superconducting and total gaps with the temperature.

order parameter in cuprate superconductors has purely *d*-wave symmetry [142, 143], but there are a wide variety of experimental data that support *s* or even more complicated types of symmetries (*d*+*s*, *d*+*is*, etc.) [144]. A more reasonable explanation is that the gap has a substantial anisotropy, while still retaining the full point-group symmetry of the crystal, and it also remains nodeless [44].

8.3.1. Properties of the Pseudogap

The existence of the pseudogap Δ_{pg} (PG) in the electronic spectra is one of the most important features of high-T_c superconductors. Several experimental results have confirmed this existence in the electronic excitation spectrum [145-147]. These experiments show that the peak of the density of states is located above the Fermi level ε_F and the separation $|\varepsilon_F - \varepsilon_{VHS}|$ is identified to the pseudogap Δ_{pg} (PG). For instance, Δ_{pg} is about 220 meV corresponding to the pseudogap transition T^* = 1050 K for La_2CuO_4, while for Y-124, Δ_{pg} is about 19 meV and T^* = 120 K [61].

For Bi-2212, the magnitude of the pseudogap is about 10 - 20 meV in low doping regime. It decreases with doping and disappears at optimal doping x_{op}. In optimally and overdoped samples with the hole concentration $x \geq 0.17$ the pseudogap is absent [148].

For bismuth compound Bi-2212, it is found that the separation $|\varepsilon_F - \varepsilon_{VHS}|$ decreases with doping [61]. This separation varies as [149]

$$\varepsilon_F - \varepsilon_{VHS} = \beta \varepsilon_F \tag{30}$$

where the parameter β control the position of the VHS with respect of the Fermi level. At optimal doping ($\beta = 0$), the Fermi level lies close to the singularity.

From this expression of the density of states, the pseudogap can be is expressed as [150]

$$\Delta_{pg}(x) = \Delta_{pg}^0 \left(1 - \frac{x}{x_{op}}\right) \tag{31}$$

In low doping regime, Δ_{pg} is large, but in intermediate doping regime, the size of the PG becomes comparable to the superconducting gap. It has been shown, that incommensurate magnetic fluctuation in yttrium compound $YBa_2Cu_3O_{6.6}$ is associated with the opening of the pseudogap in the electronic spectrum [151].

In tight-binding model, Bouvier J and Bok J have shown that the shift of the singularity from the Fermi level explains probably the pseudogap [152].

It is well established that magnetic correlations play a crucial role in the superconducting state [153] and the spin density waves (SDWs) can be considered. In conventional superconductors, charge density waves (CDWs) are produced by strong electron-phonon interaction V_p, while the spin density waves are originated by strong electron-electron repulsion V_C. The large value of V_C favors the formation of the SDW and tend to suppress superconductivity. On the other hand, the large value of V_p favors superconductivity and destroys SDW [110]. The interplay of the charge density wave (CDW), spin density wave (SDW) and superconductivity in high temperature superconductors has been studied by Panada SK and Rout GC [154]. In this model, it has been shown that in low doping regime the long range antiferromagnetic order is destroyed to give rise to SDW state accompanied by a CDW state in the system due to doping. The competition between CDW and SDW orders in underdoped $YBa_2Cu_3O_y$ has been recently studied by Hücker M and coworkers [155].

When the hole concentration x increases, the unique singularity is splitted into two singularities [61]. The separation between the two peak which is proportional to the SDW order parameter Δ_{SDW} decreases with the hole concentration [110]. We remark that the pseudogap given by Eq. (31) is proportional to the SDW parameter Δ_{SDW} ($\Delta_{pg} \propto \Delta_{SDW}$).

When the hole concentration x increases, the spin density wave parameter decreases and it is suppressed in high doping regime ($x \geq x_{op}$) giving rise to the superconductivity. It has been shown, in scaling theory [109], that the critical temperature $T_{c,SDW}$, and the SDW order parameter Δ_{SDW} are proportional to $\exp\left[\left(-(\pi^2(3.86t)/V_C\right)^{1/2}\right]$. This parameter decreases when the hole concentration x increases. In low doping regime the long range antiferromagntic order is destroyed to give rise to SDW state accompanied by a superconductivity state. In high doping regime, the SDW order is suppressed to give rise to superconductivity.

8.3.2. Properties of the Superconducting Gap

At *T* = 0, the interaction is uniquely related to the phonon V_p which is constant in the range $2\hbar\omega_D$ centered about the Fermi level ε_F and the Eq. (18) is written as

$$1 = -\frac{1}{2}\sum_{k'}\frac{V_p}{\sqrt{\varepsilon_{k'}^2 + \Delta^2(0)}} \quad (32)$$

After replacing the sum by integral, we have

$$\frac{2}{V_p} = \int_{\varepsilon_F - \hbar\varepsilon_D}^{\varepsilon_F + \hbar\varepsilon_D} \frac{n(\varepsilon)d\varepsilon}{\sqrt{(\varepsilon - \varepsilon_F)^2 + \Delta^2(0)}} \quad (33)$$

Introducing Eq. (17) in Eq. (33), we obtain

$$\frac{1}{n_1 V_p} = \int_0^{\varepsilon_F + \hbar\varepsilon_D} \frac{d\varepsilon}{\sqrt{(\varepsilon - \varepsilon_F)^2 + \Delta^2(0)}} \ln\frac{D}{\varepsilon - \varepsilon_F} + \frac{n_0}{n_1}\int_0^{\varepsilon_F + \hbar\varepsilon_D} \frac{d\varepsilon}{\sqrt{(\varepsilon - \varepsilon_F)^2 + \Delta^2(0)}} \quad (34)$$

Analytical calculation gives the following expression of the gap energy [133]

$$\Delta(0) = 2D\exp\left\{\frac{n_0}{n_1} - \left[\frac{2}{n_1 V_p} + \left(\frac{n_0}{n_1} + \ln\frac{D}{\hbar\omega_D}\right)^2 - p\right]^{\frac{1}{2}}\right\} \quad (35)$$

When there is no singularity $n_1 = 0$ and $D = \hbar\omega_D$, we have the BCS formula: $\Delta(0) = 2\hbar\omega_D \exp\left(-1/n_0 V_p\right)$. When $n_0 = 0$ and $D = \varepsilon_F = k_B T_F$ where T_F is the Fermi temperature, we obtain the expression derived by Getino *et al*:

$$\Delta(0) = 2k_B T_F \exp\left(-\left[\left(2/n_1 V_p\right) + \left(\ln\left(T_F/\theta_D\right)\right)^2 - 1.64\right]^{1/2}\right)$$

[156]. Equation (35) is applicable to low as well as high temperature superconductors. Numerical calculation shows that the gap energy $\Delta(0)$ increases when the effective mass increases. When the effective mass varies from $m^* = 2m_0$ to $m^* = 6m_0$, the gap energy increases from 4.763 meV to 17.874 meV for $\hbar\omega_D = 0.025$ eV, and from 9.546 meV to 39.80 meV for $\hbar\omega_D = 0.085$ eV. When the effective mass increases, the Fermi velocity v_F decreases while the gap energy increases. From this expression, we obtain for the parameter $\Delta(0)/D = \Delta(0)/\varepsilon_F$, the following expression

$$\frac{\Delta(0)}{\varepsilon_F} = 2\exp\left\{\frac{n_0}{n_1} - \left[\frac{2}{n_1 V_p} + \left(\frac{n_0}{n_1} + \ln\frac{D}{\hbar\omega_D}\right)^2 - p\right]^{\frac{1}{2}}\right\} \quad (36)$$

In the weak coupling limit and the Debye energy $\hbar\omega_D$ is in the range 0.035 – 0.075 eV, the ratio $\Delta(0)/\varepsilon_F$ is in the range $0.01 - 0.30$. In conventional superconductors, this ratio is very small ($\Delta(0)/\varepsilon_F \approx 10^{-4}$). The large value of this parameter has a strong impact on the number of properties of high-T_c cuprates [116, 117]. For example, a large value of this parameter leads to an unusual critical behavior near T_c. A small value of the energy Fermi with large value of the superconducting gap leads to large value of this parameter. The large value of this ratio means that a significant fraction of carriers are paired. This corresponds to small value of the Fermi velocity and large T_c.

8.4. Expressions of the Fermi Velocity and the Coherence Length

8.4.1. The Maximum of the Fermi Velocity $v_F^{\max}$

In conventional metal, the Fermi velocity is constant and it is in the range (1 - 2)10^8 cm.s^{-1}. But for the cuprate superconductors, the Fermi velocity varies from zero to its maximum value $v_F^{\max}$ given by [106]

$$v_F = \frac{\pi\hbar}{\sqrt{2}m^* a}. \quad (37)$$

The Fermi velocity decreases with the effective mass m^*. From Eq. (37), the maximum of the Fermi velocity v_F is in the range (1.072 – 3.218)10^7 cm.s^{-1} when m^* is between $2m^*$ and $6m^*$ (m_0 is the free electron mass). The small value of v_F leads to small value of the coherence length. For lanthanum compound $La_{2-x}Sr_xCuO_4$, ξ_0 is estimated between 20 Å and 40 Å. With experimental values of the superconducting gap ratio *R* and the superconducting transition temperature T_c and BCS formula of the coherence length ξ_0, we obtain the maximum of the Fermi velocity v_F in the range (1 – 1.859) 10^7 cm.s^{-1}. With Eq. (37), we obtain the same values when the effective mass m^* is large. In a previous work [150], we have shown that the average of the Fermi velocity $< v_F >$ is in the range (2 - 8)10^{-6} cms^{-1}. In the BCS theory, the coherence length is given by [131]

$$\xi_0 = \frac{\hbar v_F}{\pi\Delta(0)}. \quad (38)$$

Introducing Eq. (37) in Eq. (38), we obtain the following expression of the coherence length

$$\xi_0 = \frac{2\sqrt{2}}{\pi^2}\frac{a}{\Delta(0)/\varepsilon_F} \quad (39)$$

This formula shows that the coherence length depends on the ratio $\Delta(0)/D = \Delta(0)/\varepsilon_F$. The coherence length decreases when the ratio $\Delta(0)/\varepsilon_F$ increases. This ratio estimates what fraction of the carriers which are directly involved in the pairing. A

large gap energy and small value of the width of singularity ($D = \varepsilon_F$) contribute to the large value of this ratio. The coherence length decreases from 36 Å to 9 Å when the parameter $\Delta(0)/\varepsilon_F$ varies from 0.03 to 0.12. The possibility of having a large value of $\Delta(0)/\varepsilon_F$ and short coherence length is related to the quasi-2D structure of the high-T_c superconductors [116,117]. The large value of this parameter describes other properties such a scale of the critical region near T_c. In addition, we mention that the parameter $\left(\Delta(0)/\varepsilon_F\right)^2$ describes the shift in the dielectric function due to superconducting transition. This shift is negligibly small in conventional superconductors, but it is noticeable in high-T_c oxide superconductors [117].

Introducing Eq (36) in Eq. (39), we obtain the following expression of the coherence length

$$\xi_0 = \frac{a\sqrt{2}}{\pi^2 e^{n_0/n_1}} \exp\left[\frac{2}{n_1 V_p} + \left(\frac{n_0}{n_1} + \ln\frac{D}{\hbar\omega_D}\right)^2 - p\right]^{\frac{1}{2}}. \qquad (40)$$

The coherence length depends on the ratio n_0/n_1, on the phonon-interaction V_p, on the width of singularity *D* and on the Debye energy $\hbar\omega_D$. This expression shows that the ratio n_0/n_1 contributes to the decrease in coherence length ξ_0.

Numerical calculations show that the coherence length ξ_0 decreases, when the effective mass m^* increases. When m^* increases from $3m_0$ to $6m_0$ and V_p is in the range 0.10 – 0.14 eV, the coherence length ξ_0 decreases from 20 Å to 8 Å. When m^* varies from $3m_0$ to $6m_0$ and when the Debye energy is in the range 0.035 – 0.085 eV, the ratio ξ_0/a decreases from 7 to 2 . In this case, the coherence length ξ_0 decreases from 28 Å to 8 Å.

Other numerical calculations show that the coherence length decreases with the phonon-interaction V_p. When this interaction varies from 0.16 eV to 0.5 eV and when the Debye energy is in the range 0.035 – 0.085 eV, the ratio ξ_0/a decreases from 13.5 to 2. In this case, the coherence length ξ_0 decreases from 54 Å to 8 Å. We can see that the short coherence length in high-T_c oxides superconductors is mainly due to the large effective mass m^*. We can see also, even increase in V_p contributes to the decrease in ξ_0.

Table 5: Theoretical Values of the Coupling Constant $\lambda_p = n_1 V_p$ and the Coherence Length ξ_0 Obtained from Experimental Values of the Gap Energy for $La_{2-x}Sr_xCuO_4$ ($D = 0.5$ eV, $n_0/n_1 = 4$), for Thallium Compound Tl-2201 and Mercury Compounds Hg-1201, Hg-1212 ($D = 0.3225$ eV, $n_0/n_1 = 4$)

Compound	ξ_0 (Å) Eq. 40	$\lambda_p = n_1 V_p$ Eq. 20	$\hbar\omega_D$ (eV)	$\Delta_{\exp}(0)$ (meV)
$La_{2-x}Sr_xCuO_4$ T_c = 38 - 39 K	31.11	0.0835	0.045	17.5 Ref. 36
	31.05	0.0669	0.065	
	31.00	0.0606	0.085	
$Tl_2Ba_2CuO_{6+x}$ (Tl-2201) T_c = 92.5 K	11.10	0.2456	0.065	43 Ref. 29
	10.91	0.2273	0.075	
	10.76	0.2138	0.085	
$HgBa_2CuO_{4+x}$ (Hg-1201) T_c = 96 - 97 K	14.18	0.1988	0.065	33 Ref. 30
	13.95	0.1865	0.075	
	13.76	0.1775	0.085	
$HgBa_2CuO_{4+x}$ (Hg-1201) T_c = 96 - 97 K	10.88	0.2504	0.065	44±4 Ref. 29
	10.68	0.2315	0.075	
	10.52	0.2177	0.085	
$HgBa_2CaCu_2O_{6+x}$ (Hg-1212) T_c = 123 K	9.67	0.2814	0.065	50 Ref. 30
	9.51	0.2573	0.075	
	9.36	0.2405	0.085	

When the coupling constant is in the range 0.06 – 0.30 and the Debye energy in the range 0.025 – 0.085 eV, we obtain simultaneously the experimental values of the gap energy $\Delta(0)$ and the coherence length ξ_0 (Table **5**). The properties of the coherences length ξ_0 and the superconducting gag $\Delta(0)$ for hole-doped superconductors are studied in more detail in Ref. 106. With experimental values of the superconducting gap ratio R and the superconducting transition temperature T_c and BCS formula of the coherence length ξ_0, we obtain the Fermi velocity v_F in the range (1 – 1.859) 10^7 cm.s^{-1}.

8.4.2. The Average of the Fermi Velocity $< v_F >$

It is interesting to calculate the coherence length with the average of the Fermi velocity $< v_F >$. This average of v_F is given by

$$\hbar < v_F >= \frac{\hbar \int v_F n(k) dk}{\int n(k) dk} \tag{41}$$

where $n(k)$ is the density of states and v_F the Fermi velocity given by

$$v_F = \frac{1}{\hbar} \frac{d\varepsilon}{dk_\perp}. \tag{42}$$

Introducing Eq. (42) in Eq. (41), we obtain

$$\hbar < v_F >= \frac{a^2}{4\pi^2} \frac{\int_{-\Delta}^{+\Delta} d\varepsilon \int dk}{\int_{-\Delta}^{+\Delta} n(\varepsilon) d\varepsilon}. \tag{43}$$

Finally, we obtain

$$< v_F >= \frac{\sqrt{2} a 2D}{\pi\hbar} \frac{1}{\left[1 + \frac{n_0}{n_1} + \ln\frac{D}{\Delta}\right]}. \tag{44}$$

With this formula, we obtain small values of the Fermi velocity. Our calculation shows that the average value of v_F is in the range (2 - 8)10^6 cm.s^{-1}. The small value of the Fermi velocity is one the features of the cuprates. These values are smaller than those obtained from the maximum of the Fermi velocity. In conventional metal, the Fermi velocity is in the range (1 - 2)×10^8 cm.s^{-1}. The small value of the average of the Fermi velocity leads to small values of the coherence length ξ_0, although the higher T_c also contributes to the decrease in ξ_0. Introducing Eq. (36) in Eq. (44) with $D = \varepsilon_F$, we obtain

$$\xi_0 = \frac{a\sqrt{2}}{\pi^2 e^{n_0/n_1}} \frac{\exp\left[\frac{2}{n_1 V_p} + \left(\frac{n_0}{n_1} + \ln\frac{D}{\hbar\omega_0}\right)^2 - p\right]^{\frac{1}{2}}}{c + \left[\frac{2}{n_1 V_p} + \left(\frac{n_0}{n_1} + \ln\frac{D}{\hbar\omega_0}\right)^2 - p\right]^{\frac{1}{2}}} \tag{45}$$

where $c = 0.3068$. This expression depends on the phonon interaction, on the width of singularity *D*, on the vibrational energy $\hbar\omega_0$ and on the ratio n_0 / n_1. Numerical calculation shows that ξ_0 decreases when the effective mass carriers m^* increases. The coherence length decreases with the coupling constant $\lambda_p = n_1 V_p$. When the coupling constant λ_p increases from 0.06 to 0.173, the coherence length decreases from 45.59 Å to 8 Å for $n_0 = 0$ and it decreases from 24.8 Å to 8 Å for $n_0 = n_1$ ($D = 0.645$ eV, $\hbar\omega_0 = 0.045$ eV, Figure **9**). In weak coupling limit (λ_p = 0.06 – 0.173), we obtain small values of coherence length ξ_0 (8 – 25 Å). These values are in good agreement with experimental results.

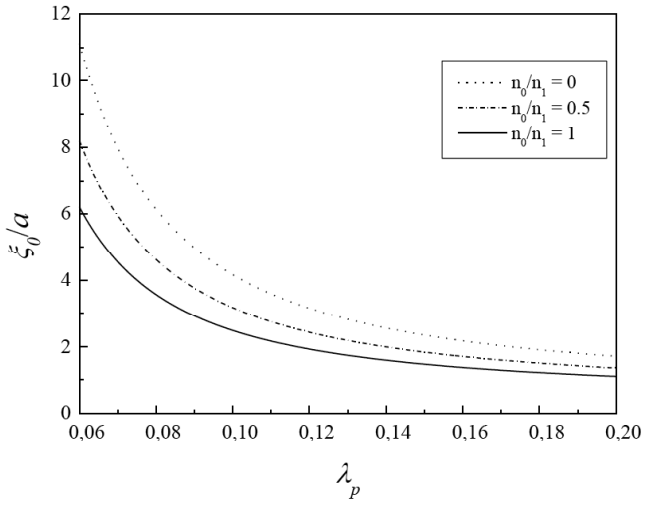

Figure 9: Variation of the coherence length with coupling constant for different value of the ration n_0 / n_1.

These values are obtained in a Fermi-liquid theory [116, 120]. In this theory the major normal and superconducting parameters of high-T_c cuprates have been evaluated. For lanthanum compound $La_{2-x}CuO_4$, one obtained: $\varepsilon_F = 0.1$ eV, $m = 0.5 m_0$, $v_F = 8 \times 10^6$ cm.s^{-1} and $\xi_0 = 20$ Å.

8.5. The Superconducting Gap Ratio

The high-T_c superconductors are characterized by a large value of the superconducting gap ratio $R = 2\Delta(0)/k_B T_c$. This ratio has an ordinary magnitude 3.53 in conventional superconductors, but it is much larger, being 5 - 13 for the new superconductors. The large gap ratio is expected to be associated with strong anisotropy [44]. The large value of this parameter is still not understood. Various approaches based on electronic as well as phonon-based interaction, sometimes for isotropic *s*-wave and other times for *d*-wave pairing, have been proposed to explain the large value of R [156-165] but the maximum values of this parameter are still much lower than the experimental results. At low temperature the attractive interaction is due essentially to the phonons and the superconducting gap ratio is close to the BCS value $R_{BCS} = 3.53 - 3.99$ for s-wave and from 4 to 5 for *d*-wave. This is a very small variation between R_d and R_s ($R_d - R_s \approx 1 - 1.47$). Both in *s*-wave and in *d*-wave, the theoretical values are still smaller than experimental values.

In Jahn-Teller model [123], one obtain large value of the superconducting gap ratio R: $3.53 \le R \le 7$. These values are greater than the BCS value 3.53 but are still smaller than experimental results ($\approx 7 - 13$) of the hole-doped cuprates.

In a strong coupling method based on a Fermi-liquid approach, on obtain the maximum R of order of ≈ 5. The strong coupling is not sufficient to give the high experimental value of the superconducting gap ratio R [116].

In two-dimensional charges density waves (CDWs), the superconducting gap ratio R varies very little from the BCS value 3.53 [165]. Large values of R ($\approx 5 - 8$) can be obtained in CDW model [166]. These theoretical values are still smaller than experimental values.

The expression of the superconducting gap ratio R is obtained by using Eqs (25) and (35)

$$R = R_{BCS} \exp\left\{ \left[A - B\right]^{\frac{1}{2}} - \left[\frac{2}{n_1 V_p} + \left(\frac{n_0}{n_1} + \ln \frac{D}{k_B \theta_D} \right)^2 - p \right]^{\frac{1}{2}} \right\} \tag{46}$$

where A and B are given by the Eqs. (26) and (27) respectively. This expression is applicable to the cuprates as wall as the conventional superconductors. In low temperature, there is no magnetic excitations ($V_m = 0$) and Eq. (46) leads to $R = R_{BCS} = 3.53$. At high temperature, the attractive interaction is related only to magnetic excitations and equations (23) and (35) lead to the following expression of the superconducting gap ratio R

$$R = R_{BCS} \exp\left\{ \left[\frac{2}{n_1 V_m} + \left(\frac{n_0}{n_1} \right)^2 - p \right]^{\frac{1}{2}} - \left[\frac{2}{n_1 V_p} + \left(\frac{n_0}{n_1} + \ln \frac{D}{\hbar\omega_0} \right)^2 - p \right]^{\frac{1}{2}} \right\} \tag{47}$$

The parameter R lies close the BCS value when

$$\lambda_p = \frac{\lambda_m}{1 - \lambda_m \left[\frac{n_0}{n_1} \ln \frac{D}{k_B \theta_0} + \frac{1}{2} \left(\ln \frac{D}{k_B \theta_0} \right)^2 - 0.16 \right]} \tag{48}$$

To have this ratio greater than the BCS value, the coupling constant λ_p must be greater than the coupling constant related the magnetic excitations λ_m. Numerical calculation shows that when the coupling constant λ_p increases from 0.079 to 0.120, the superconducting gap ratio *R* increases from the 5.99 to 13.18 for $\lambda_m = 0.048$ corresponding to T_c = 88.14 K, and increases from 3.53 to 9 for $\lambda_m = 0.054$ corresponding to T_c = 114.47 K (*D* = 0.645, n_0/n_1 = 2 and $\hbar\omega_0 = 0.045$ eV). We remark that even weak interaction can produce a large effect on the superconducting gap ratio *R*. For example, when λ_m varies from 0.048 to 0.054 ($\Delta\lambda_m$ = 0.006), *R* varies from 13.18 to 9 (ΔR = 4.18).

In a previous work [150] we have shown that when λ_p varies from 0.0725 to 0.120, *R* increases from the BCS value 3.53 to 9 for $\hbar\omega_0 = 0.045$ eV, and from 5 to 13.69 for $\hbar\omega_0 = 0.085$ eV ($D = 0.645$ eV and $\lambda_m = 0.05$). Figures **10** and **11** show that the superconducting gap ratio R increases when the effective mass m^* increases. When the effective mass increases from $2m_0$ to $6m_0$, R increases from 4.47 to 9.10 for $\hbar\omega_D = 0.035$ eV and from 7.47 to 13.74 for $\hbar\omega_D = 0.075$ eV (Figure **10**). For $m^* = 6m_0$, the superconducting gap ratio R increases from 10.85 to 16.90 when the coupling constant $\lambda_p = n_1 V_p$ varies from 0.11 to 0.14 (Figure **11**). At low temperature, our calculation shows that the superconducting gap ratio *R* is equal to the BCS value 3.53. This parameter is exactly evaluated numerically and it is found to be larger than 3.53. The value of R lies in the range 3.53 – 4 when the Fermi level lies close to the van Hove singularity. In *d*-wave symmetry, the superconducting gap ratio R_d is still significantly enhanced from the BCS value 3.53. The

maximum value of R is ≈ 5 when $\omega_0 / T_c \to 0$ and the minimum value is predicted to be 4.3 in the limit $\omega_0 / T_c \to \infty$. The maximum value of *R* in *d*-wave symmetry [161] is still much lower than experimental values.

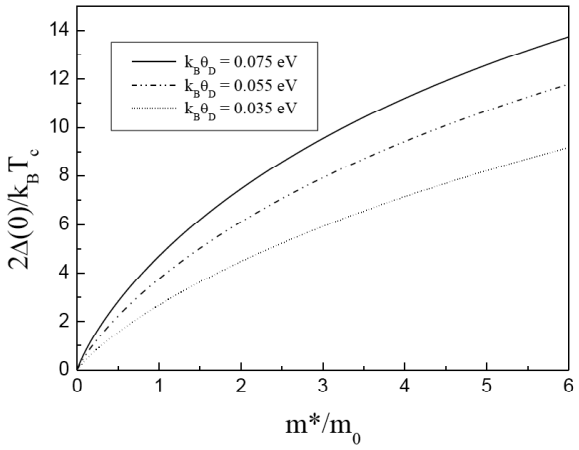

Figure 10: Variation of the superconducting gap ratio with the effective mass m^* for different values of the Debye energy ($n_0 / n_1 = 1$, $\lambda_m = 0.06$ and $\lambda_p = 0.12$).

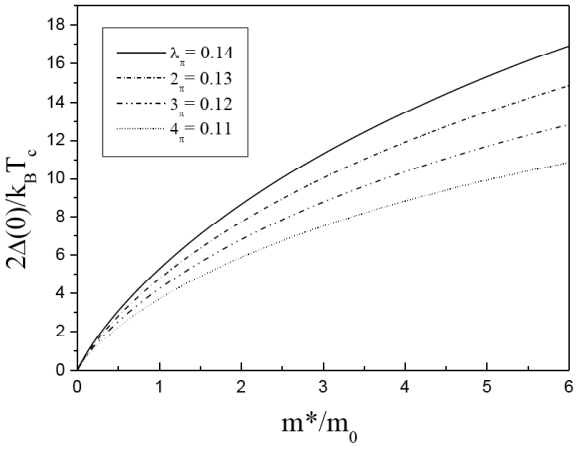

Figure 11: Variation of the superconducting gap ratio with the effective mass m^* for different values of the coupling constant $\lambda_p = n_1 V_p$ ($n_0 / n_1 = 1$, $\lambda_m = 0.06$ and $k_B\theta_D = 0.065$ eV).

In order to have high-T_c (38 –135 K), experimental values of the gap energy and large values of the superconducting gap ratio, the coupling constant due to the magnetic excitations λ_m must be smaller than that corresponding to the phonons λ_p.

Numerical calculations show that when λ_m is in the range 0.020-0.060 and λ_p is in the range 0.03 0.12, the superconducting gap ratio R varies from the BCS value to 13. These values are in good agreement with experimental results (Tables **6** and **7**).

8.6. Properties of the Isotope Effect

The high-T_c cuprates such $YBa_2Cu_3O_{6+x}$ and B-Sr-Ca-Cu-O systems are characterized by a small isotope coefficient α. This coefficient depends strongly on the hole concentration x and can significantly exceed the BCS limit in low doping regime. When the concentration increases, the superconducting transition $T_c(x)$ increases and reaches its maximum at optimal doping x_{op}, while the isotope coefficient α decreases and reaches its minimum at x_{op}.

The isotope coefficient α is in the range 0.4-0.8 in low doping regime whereas it is almost negligible in high doping regime. In the absence of doping, the CuO_2 plane has strong antiferromagnetic correlation and the insulating antiferromagnetic state is converted into a metallic paramagnetic one with doping. The isotope coefficient α which is maximum at the border to the antiferromagnetic state decreases with doping and takes small value at optimal doping. The large value of α in low doping regime reveals the role played. The small value of α in high doping regime leads to suggestion that the attraction between electrons or holes might be related to another mechanism with possible phononic contribution.

The quasi-2D structure of the cuprates leads naturally to a van Hove singularity (VHS) in the density of states. In this scenario, various approaches have attempted to explain the anomalous behavior of the isotope effect in high-T_c superconductors [106, 110, 136, 163-165]. Other works have tried to explain the small value of this coefficient [167-170] In all these works, it has been considered only the phonon interaction.

In the van Hove scenario both in weak and strong coupling, one obtain small values of the isotope coefficient, but these values are still larger than experimental values.

In the van Hove scenario, with a weak coupling model of charge density wave CDW, the isotope coefficient can become very small [165] in comparison with $0.5 > \alpha_{CDW(BF)} > 0.39$ for Balseiro-Falicov model [171]. In all these models only the electron-phonon interaction has been considered.

In the interacting hole spin model, one obtain small value of the isotope coefficient corresponding to the maximum T_c. For yttrium compound $YBa_2Cu_3O_{6+x}$, the calculated value of α is consistent with experimental value ≈ 0.02 [6]. In this model, only the magnetic interaction has been considered.

Table 6: Theoretical Values of the Coupling Constant $\lambda_p = n_1 V_p$, Gap $\Delta(0)$ and Superconducting Gap Ratio $R = 2\Delta(0)/k_B T_c$ for Some Cuprate Superconductors for Different Values of the Debye Energy ($D = 0.625$ eV and $n_0/n_1 = 3$)

Compound	$k_B\theta_D$ (eV)	$\Delta(0)$ (meV) Eq. (35)	λ_p Eq. (35)	$R = 2\Delta(0)/k_B T_c$ Eq. (47)
$La_{2-x}Sr_xCuO_4$ 38 (K)	0.025	13.022	0.099	7.95
	0.045	14.806	0.079	9.03
	0.065	15.820	0.071	9.65
$YBa_2Cu_3O_7$ 92 (K)	0.025	20.777	0.150	5.24
	0.045	23.045	0.106	5.81
	0.065	25.560	0.093	6.44
$Bi_2Sr_2CaCu_2O_8$ 84 (K)	0.055	35.073	0.130	9.68
	0.065	36.500	0.120	10.07
	0.075	37.133	0.112	10.25
$Bi_2Sr_2Ca_2Cu_3O_{10}$ 110 (K)	0.065	45.275	0.144	9.54
	0.075	46.393	0.133	9.77
	0.080	47.630	0.130	10.04

Table 7: Theretical Values of the Coupling Constants λ_m and λ_p Obtained from Experimental Values of T_c and $\Delta(0)$ for Mercury Compounds

Compound	λ_m Eq. (23)	T_c (K)	λ_p Eq. (35)	$\Delta(0)$ (meV)	$R = 2\Delta(0)/k_B T_c$
Hg-1201	0.0260	97	0.0754	33	7.9 Ref. 30
Hg-1212	0.0277	123	0.1076	50	9.5 Ref. 30
Hg-1223	0.0285	135	0.1789	75	13 Ref. 30

To study the isotope effect, we consider the variation of the superconducting transition temperature T_c when varying θ_D. We know that θ_D varies like $M^{-1/2}$ and the isotope coefficient as defined in the expression $T_c \propto M^{-\alpha}$, can be calculated from the following expression

$$\alpha = -\frac{\partial \ln T_c}{\partial \ln M} = \frac{1}{2}\frac{\partial \ln T_c}{\partial \ln \theta_D} \tag{49}$$

To determine the coefficient α, we differentiate Eq. (25) with respect to θ_D. An exact expression of α is obtained

$$\alpha = \frac{1}{2}\frac{\left[\frac{n_0}{n_1} + \ln\frac{D}{k_B\theta_D}\right]\left(1 - \frac{V_m}{V_p + V_m}\right)}{\left[A - B\right]^{\frac{1}{2}}} \tag{50}$$

where A and B are given by the Eq. (26) and Eq. (27) respectively. We can write Eq. (50) as

$$\alpha = \frac{1}{2}\frac{\left[\frac{n_0}{n_1} + \ln\frac{D}{k_B\theta_D}\right]}{\left[\frac{n_0}{n_1} + \ln\frac{1.13D}{k_B T_c}\right]}\left(1 - \frac{V_m}{V_p + V_m}\right) \tag{51}$$

For the new superconductors and in absence of the magnetic excitations, we find the expression of α obtained in a previous work [133]. In this case, we remark that this coefficient decreases from 0.34 to 0.32 when phonons energy varies from 0.025 eV to 0.065 eV. These values are well over the experimental data ($0 - 0.02$) for the high-T_c superconductors. In this situation, we distinguish the limiting cases

1. for $n_0 = 0$, two cases are possible, (a) when $D = \varepsilon_F$ this leads to an exact result than obtained by Tsuei *et al* [135], when $D = 21.177796t$, we have the expression obtained by Szczesniak *et al* [136]

2. for $n_0 = (1/2\pi^2 t)\ln 4$ and $D = \varepsilon_F = 4t$, we obtain the expression derived by Xing *et al* [108].

In all these cases, phonon energy reduces the isotope coefficient α, but the values obtained by these formulas are still larger than experimental results.

Equation (50) is a general expression describing the properties of the isotope effect for high-T_c superconductors. Numerical calculations show that the isotope coefficient decreases with the superconducting transition temperature T_c in qualitative agreement with experimental [49-56] and numerical results [110] (Figures **12** and **13**). When the temperature increases this coefficient decreases from $\alpha_p \approx 0.38 - 0.42$ to its minimum value $\alpha_m \approx 0.006 - 0.05$. The origin of this behavior is related to the attractive interaction due to the magnetic excitation and phonons. In the absence of the magnetic excitations α is large and T_c is low. On the other hand, when we neglect the electron-phonon interaction α is zero and T_c is large. Yndurain has studied the variation of the isotope coefficient with hole concentration, considering spin density wave SDW in two-dimensional system. In this model, he has found that α varies abruptly near the hole concentration where T_c is maximum and he has shown that α decreases with T_c. When the SDW is large, the density of states varies very rapidly near the Debye frequency and therefore the isotope effect is large and when the SDW is small or zero the isotope effect is negligible.

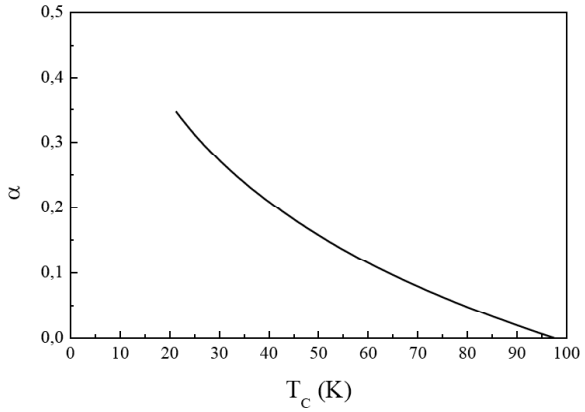

Figure 12: Variation of the isotope coefficient α with the superconducting transition temperature T_c ($D = 0.714$ eV, $k_B\theta_D = 0.065$ eV, $n_0/n_1 = 6$ and $\lambda = 0.026$).

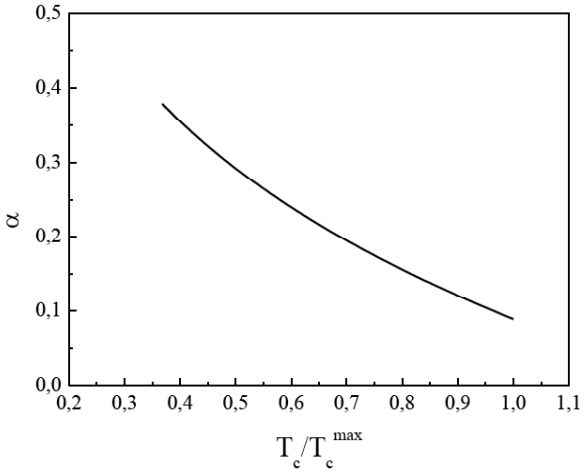

Figure 13: Variation of the isotope coefficient with $T_c/T_c^{\max}$ with $D = 0.5$ eV, $k_B\theta_D = 0.085$ eV, $n_0/n_1 = 9$ and $\lambda = 0.026$.

In Jahn-Teller model [123], one obtains both positive and negative value of the isotope coefficient α. The values of α are in good agreement with experimental data for the lanthanum and yttrium compounds. This model explains some negative values observed in high-T_c oxides.

9. SUMMARY

The high-T_c cuprate superconductors such $La_{2-x}Sr_xCuO_4$ and $YBa_2Cu_3O_{6+x}$ are antiferromagnetic insulators in low doping regime. Upon hole doping, the antiferromagnetic order rapidly disappears and the system becomes a superconductor. In these compounds the magnetic correlations persist and are still present at optimal doping x_{op}. The occurrence of superconductivity is obtained only after the complete destruction of the three-dimensional AF order. In these compounds, there is a coexistence between superconductivity and two-dimensional antiferromagnetic 2D-AF, characterized by a short magnetic correlation length decreasing with x. This indicates that the magnetic correlations survive in the highest T_c.

The superconducting transition temperature $T_c(x)$ increases with hole concentration and reaches its maximum at optimal doping x_{op}. The overdoped state is characterized by a drastic decrease in T_c upon overdoping. Additional increase in hole doping leads to a total suppression in superconductivity.

The electronic properties of these new compounds are almost two-dimensional. All high-T_c superconductors are anisotropic and the good conductivity occurs essentially in the CuO_2 planes. The

Cooper pairs are concentrated near CuO_2 planes and propagate along these planes. The nearly 2D electronic structure leads to van Hove singularities in the density of states coinciding with a saddle point in $\varepsilon(k)$ surface. The peak of the density of states is located above the Fermi level ε_F and the separation $|\varepsilon_F - \varepsilon_{VHS}|$ is identified to the pseudogap Δ_{pg} (PG). When the Fermi level coincides with the singularity, a band Jahn-Teller is expected which leads to a structural phase transition from the tetragonal phase to an orthorhombic one. The unique van Hove singularity of the tetragonal phase is splitted into two singularities with the Fermi level lying between them, in a region where the density of states is low. The separation between the two singularities $|\varepsilon^1_{VHS} - \varepsilon^2_{VHS}|$ is proportional to the SDW order Δ_{SDW}.

At optimal doping the VHS is close to the Fermi level ε_F in all cuprate superconductors. The separation $\varepsilon_F - \varepsilon_{VHS} = \beta\varepsilon_F$ which is identified to the pseudogag Δ_{pg}, is suppressed to zero at optimal doping x_{op} ($\beta = 0$).

The electrical resistivity $\rho_{ab}(T)$ varies with doping. At optimal doping, the cuprate superconductors are characterized by a T-linear resistivity that survives for all $T > T_c$. This linearity of the resistivity is a universal feature confirming that it is intrinsic to the CuO_2 planes. In low doping regime, the resistivity deviates from linearity at much higher T and its value decreases with hole concentration in a manner similar to $\Delta_{pg}(x)$. It seems that there is a correlation between the electrical resistivity and the pseudogap.

The Hall constant R_H of hole-doped cuprates varies markedly with both x and T. There is a symmetrical change in sign of the Hall constant both in hole doped $La_{2-x}Sr_xCuO_4$ and electron doped $Nd_{2-x}Ce_xCuO_4$. These two compounds are symmetrical with regard to the change in the mechanism conduction with composition. The superconductivity is obtained near the crossover region of the sign.

In low doping regime, the Hall constant varies as: $R_H(x) \approx 1/x$. When the doping increases, the compound becomes metallic and the Hall constant deviates from the curve expected [20].

The Hall constant $R_H(T)$ decreases with the temperature T. At optimal doping this coefficient varies as: $R_H(T) \approx 1/T$. It appears that there is a correlation between the electrical resistivity, the Hall constant and the pseudogap Δ_{pg}.

The total gap $\Delta(T) = \sqrt{\Delta^2_{sg}(T) + \Delta^2_{pg}(T)}$ is nearly constant and consistent with experimental results. At low temperature, the total gap becomes a pure SC gap, but at high temperature it is a pure pseudogap ($T_c < T < T^*$), and at intermediate temperatures the gap has two contributions, one form the superconducting gap and the other form the pseudogap. This pseudogap $\Delta_{pg}(x)$ decreases with doping x and it is suppressed to zero at optimal doping x_{op} while the superconducting gap Δ_{sg} increases and reaches its maximum at x_{op}. This pseudogap can be described by CDW state or SDW. The significance of the various forms of CDW (Δ_{CDW}) and SDW (Δ_{SDW}) is still not understood. Their detection, characterization and relationship with superconductivity remain open problems.

There are two superconducting gaps: Δ^s with s-wave symmetry and Δ^d with d-wave symmetry. The presence of the two superconducting condensates with different symmetries s and d in high-T_c superconductors has been suggested by Muller [172, 173] and confirmed by experimental results for $La_{1.83}Sr_{0.17}CuO_4$ [174]. Experimentally, the ARPES spectra consist of two kinds of gap: a large smooth pseudogap and a relatively sharp small gap which exists in the $p+ip$ superconducting region only [175]. The pseudogap survives to very high temperatures whereas the much smaller $p+ip$ superconducting gap does not. The pseudogap state and the superconducting state is recently discussed in mean field theory [176].

In the weak coupling limit ($\lambda_p \approx 0.03 - 0.12$), we obtain simultaneously large value of the gap energy and small values of the coherence length ξ_0. The values obtained in this model are in good agreement with experimental results.

Our calculations show that the Fermi energy is in the range 0.1 – 1 eV, the Fermi velocity is in the range $(2 - 8)10^{-6}$ cms^{-1} and the coherence length ξ_0 is of order of $\approx 08 - 20$ Å.

In order to have small value of the Fermi velocity and short coherence length, the effective mass tends to be large.

In the Fermi liquid approach, one obtain the same values of these parameters. For example, one obtain the Fermi energy $\varepsilon_F \approx 0.1$ eV, the Fermi velocity $v_F \approx 8\times10^6$ cms^{-1}, and the effective mass $m^* \approx 5m_0$.

Our numerical calculations show that when λ_m is in the range 0.020 - 0.06 and λ_p is in the range 0.03 - 0.12, the superconducting gap ratio R varies from the BCS value to 13. The superconducting gap ratio $R = 2\Delta(0)/k_B T_c$ increases with the superconducting transition temperature T_c. The values of R are in good agreement with experimental data. Recently it has been found that the superconducting gap energy is correlated with the value of the pseudogap temperature T^* [177]. On the other hand, no correlation between 2Δ(0) and the critical temperature T_c has been found. These values mean that $R = 2\Delta(0)/k_B T_c$ can vary very strongly together with the chemical composition, while the parameter $R = 2\Delta(0)/k_B T^*$ does not change significantly.

The isotope coefficient decreases with T and reaches its minimum at optimal doping. At low temperature the isotope coefficient is large but at high temperature this coefficient is very small. When the superconducting transition temperature T_c increases the isotope coefficient α decreases from its maximum value $\alpha_p \approx 0.38 - 0.40$ to its minimum value $\alpha_m \approx 0.006 - 0.05$. These values are in qualitative agreement with experimental results.

In the Jahn-Teller model, one obtain high T_c and large value of the superconducting gap ratio $\approx 3.53 - 7$. In this model [123], one obtains both positive and negative value of the isotope coefficient α. The values of α are in good agreement with experimental data for the lanthanum and yttrium compounds. This model explains some negative values observed in high-T_c oxides. It seems the electron-doped superconductors are very described in this model.

It is interesting to develop the JT model in the van Hove scenario and compare with our results.

In conclusion, we have obtained general expressions for the superconducting gap ratio R and the isotope effect α which have been derived with the van Hove singularity in the weak coupling case. These expressions are applicable to the cuprates as well as the conventional superconductors. At low temperature, we obtain the experimental values of R ($\approx 3.53 - 6$) and α (≤ 0.05) for the electron-doped superconductors. At high temperature, we obtain large value of R ($\approx 7 - 13$) and small value of α ($\approx 0.006 - 0.05$). These values are in good agreement with experimental results for the hole-doped superconductors. Based on our results, we predict that these two parameters are correlated with the pseudogap temperature T^*. The Fermi velocity v_F and the coherence length ξ are also evaluated and discussed in more detail.

The competition between phonons and magnetic excitations, in the van Hove scenario, can provide a basis for understanding the high T_c, large superconducting gap ratio R and small isotope coefficient α, and possibly the origin of high-temperature superconductivity.

AKNWLEDGMENTS

I am pleased to have this paper appear in the Special Issue “High Temperature Superconductivity: Theory and Experiment”. I am very grateful to Profs Bouvier J, Bok J, Markiewicz RS, Brandow B, Krezin VZ and Apostol M for sending their interesting papers.

REFERENCES

[1] Bednorz JG, Müller KA. Possible high superconductivity in the Ba-La-Cu-O system. Z Phys B. 1986; 64(2): 189-193. http://dx.doi.org/10.1007/BF01303701

[2] Anderson PW. The resonating valence bond state in La_2CuO_4 and superconductivity Science. 1987; 235(4793): 1196-1198. http://dx.doi.org/10.1126/science.235.4793.1196

[3] Labbé J, Bok J. Superconductivity in alkaline-earth-substituted La_2CuO_4: a theoretical model. Europhys Lett. 1987; 3(11): 1225-1230. http://dx.doi.org/10.1209/0295-5075/3/11/012

[4] Aoki H and Kamimura H. Jahn-Teller-effect mediated superconductivity in oxides. Solid State Commun. 1987; 63(7): 665-669. http://dx.doi.org/10.1016/0038-1098(87)90876-3

[5] Apostol M. On the mechanism of high-temperature superconductivity in Ba-La(Y)Cu-O type systems. Solid State Commun. 1988; 67(4): 425-429. http://dx.doi.org/10.1016/0038-1098(88)91059-9

[6] Kurihara S. Interacting hole-spin model for oxide superconductors. Phys Rev B. 1989; 39(10): 6600-6606. http://dx.doi.org/10.1103/PhysRevB.39.6600

[7] Johnson KH, Clougherty DP and McHenry ME. Dynamic Jahn-Teller coupling anharmonic oxygen vibrations and high-superconductivity in oxides. Mod Phys Lett B. 1989; 3(18): 1367-1374. http://dx.doi.org/10.1142/S0217984989002065

[8] Englman R, Halperin B and Weger M. Jahn-Teller (reverse sign) mechanism for superconductive pairing. Physica C. 1990; 169(3-4): 314-324. http://dx.doi.org/10.1016/0921-4534(90)90193-I

[9] Fil DV, Tokar OI, Shelankov AL and Weber W. Lattice-mediated interaction of Cu2+ Jahn-Teller ions in insulating cuprates. Phys Rev B. 1992; 45(10): 5633-5640. http://dx.doi.org/10.1103/PhysRevB.45.5633

[10] Rabinowtz M and McMullen T. Phenomenological theory of cuprate superconductivity. App Phys Lett. 1993; 63(7): 985-986 http://dx.doi.org/10.1063/1.109866

[11] Chubukov AV and Morr DK. Electronic structure of underdoped cuprates. Phys Rep 1997; 288(1-6): 355-387. http://dx.doi.org/10.1016/S0370-1573(97)00033-1

[12] Cho JH, Borsa F, Johnston DC and Torgeson DR. Spin dynamics in $La_{2-x}Sr_xCuO_4$ ($0.02 \leq x \leq 0.08$) from La139 NQR relaxation: Fluctuations in a finite-length-scale system. Phys Rev B 1992; 46(5): R3179-R3182. http://dx.doi.org/10.1103/PhysRevB.46.3179

[13] Kitazawa A. Electronic structures of oxide superconductors – Development of concepts. Earlier and Recent Aspects of Superconductivity, edited by Bednorz JG and Müller KA. 1991; 45-65.

[14] Tranquada JM. Magnetic and electronic correlations in $YBa_2Cu_3O_{6+x}$. Earlier and Recent Aspects of Superconductivity, edited by Bednorz JG and Müller KA. 1991; 422-440.

[15] Germain P and Labbé J. Orthorhombicity, anitiferromagnetism and superconductivity in $YBa_2Cu_3O_{6+x}$. Europhys Lett. 1993; 24(5): 391-396. http://dx.doi.org/10.1209/0295-5075/24/5/012

[16] Burger JP and Zanoun Y. Main properties and origin of the new high- superconductors. Materials Chemistry and Physics. 1992; 32(1): 177-182. http://dx.doi.org/10.1016/0254-0584(92)90274-C

[17] Tallon JL, Bernhard C, Shaked H, Hitterman RL and Jorgensen JD. Generic superconducting phase behavior in high- cuprates: variation with hole concentration in $YBa_2Cu_3O_{7-\delta}$ Phys Rev B. 1995; 51(18): R12911-R12914. http://dx.doi.org/10.1103/PhysRevB.51.12911

[18] Markiewicz RS, Sahrakorpi S, Lindroos M, Lin H and Bansil A. One-band tight- banding model parametrization of the high- cuprates including the effect dispersion. Phys Rev B. 2005; 72(5): 054519-054531. http://dx.doi.org/10.1103/PhysRevB.72.054519

[19] Fisher RA, Gordon JE and Phillips NE. High-Superconductors: Thermodynamic Properties. HandBook of High-Temperature Superconductivity. Theory and Experiment, edited by John Robert Shrieffer 2006; 345-397.

[20] Hussey NE. Normal State Transport Properties. HandBook of High-Temperature Superconductivity. Theory and Experiment, edited by John Robert Shrieffer 2006; 399-425.

[21] Hussey NE, Takagi H, Tajima S, Rykov AI and Yoshida K. Charge confinement on the CuO_2 planes in slightly overdoped $YBa_2Cu_3O_{7-\delta}$ and the role of metallic chains. Phys Rev B 2000; 61(10) R6475-6478. http://dx.doi.org/10.1103/PhysRevB.61.R6475

[22] Kadowaki K, Li JN and Franse JJM. Superconducting fluctuation effects on the magnetoconductivity in single-crystalline $YBa_2Cu_3O_{7-\delta}$ and $Bi_2Sr_2CaCu_2O_{8+\delta}$. J. Magn. Magn. Mater.1990; 90-91: 678-680. http://dx.doi.org/10.1016/S0304-8853(10)80247-1

[23] Boebinger GS, Ando Y, Passner A, Kumira T, Okuya M, Shimoyama J *et al*. Insulator- to-Metal Crossover in the Normal State of $La_{2-x}Sr_xCuO_4$. Near Optimum Doping. Phys Rev Lett. 1996: 77(27): 5417-5420. http://dx.doi.org/10.1103/PhysRevLett.77.5417

[24] Ono S, Ando Y. Evolution of the resistivity anisotropy in $Bi_2Sr_{2-x}La_xCuO_{6+\delta}$ single crystals for a wide range of hole doping. Phys Rev B. 2003; 67(10): 104512-9. http://dx.doi.org/10.1103/PhysRevB.67.104512

[25] Giura M, Fastampa R, Sarti S, and Silva. Normal-state c-axis transport in $Bi_2Sr_2CaCu_2O_{8+\delta}$. Interlayer tunneling and thermally activated dissipation. Phys Rev B 2003; 68(13); 134505-7. http://dx.doi.org/10.1103/PhysRevB.68.134505

[26] Manako T, Kubo Y and Shimakawa Y. Transport and structural study of $Tl_2Ba_2CuO_{6+\delta}$ single crystals prepared by the KCl flux method. Phys Rev B 1992; 46(17): 11019-11024. http://dx.doi.org/10.1103/PhysRevB.46.11019

[27] Ekino T, Doukan T, Fujii H, Nakamura F, Sakita S, Kodama M *et al*. Superconducting energy gap of $La_{1.85}Sr_{0.15}CuO_4$ single crystals from break-junction tunneling. Physica C 1996; 263(1-4): 249-252. http://dx.doi.org/10.1016/0921-4534(95)00714-8

[28] Ekino T and Akimitsu J. Energy gaps in Bi-Sr-Ca-Cu-O and Bi-Sr-Cu-O systems by electron tunneling. Phys Rev B 1989; 40(10): 6902-6911. http://dx.doi.org/10.1103/PhysRevB.40.6902

[29] Yu G, Li Y, Motoyama EM and Greven M. A universal relationship between magnetic resonance and superconducting gap in unconventional superconductors. Nature Phys 2009; 5: 873-875. http://dx.doi.org/10.1038/nphys1426

[30] Wei JYT, Tsuei CC, van Bentum PJM, Xiong Q, Chu CW and Wu MK. Quasiparticle tunneling spectra of the high-Tc mercury cuprates: Implications of the d-wave two-dimensional van Hove scenario. Phys Rev B 1998; 57(6): 3650-3662. http://dx.doi.org/10.1103/PhysRevB.57.3650

[31] Lee WS, Vishik IM, Tanaka K, Lu DH, Sasagawa T, Nagaosa N *et al*. Abrupt onset of a Second energy gap at the superconducting transition of underdoped Bi2212. Nature (London). 2007; 450: 81-84. http://dx.doi.org/10.1038/nature06219

[32] Schachinger E and Carbotte JP. Coupling to spin fluctuations from conductivity scattering rates. Phys Rev B 2000; 62(13): 9054-9058. http://dx.doi.org/10.1103/PhysRevB.62.9054

[33] Guyard W, Sacuto A, Cazayous M, Gallais Y, Le Tacon M, Colson D *et al*. Temperature dependence of the gap size near the Brillouin-zone nodes of $HgBa_2CuO_{4+\delta}$ superconductors. Phys Rev Lett 2008; 101(9): 097003-4. http://dx.doi.org/10.1103/PhysRevLett.101.097003

[34] Fedorov AV, Valla T, Johnson PD, Li Q, Gu GD and Koshizuka N. Temperature dependent photoemission studies of optimally doped $Bi_2Sr_2CaCu_2O_8$. Phys Rev Lett 1999; 82(10): 2179-2182. http://dx.doi.org/10.1103/PhysRevLett.82.2179

[35] Ideta S, Takashima K, Hashimoto M, Yoshida T, Fujimori A, Anzai H *et al*. Enhanced superconducting gaps in the trilayer high-temperature $Bi_2Sr_2Ca_2Cu_3O_{10+\delta}$ cuprate superconductor. Phys Rev Lett 2010; 104(22): 227001-4. http://dx.doi.org/10.1103/PhysRevLett.104.227001

[36] Yoshida T, Hashimoto M, Ideta S, Fujimori A, Tanaka K, Mannella N *et al*. Universal versus material-dependent two-gap behaviors of the high- cuprate superconductors: angle-resolved photoemission study of $La_{2-x}Sr_xCuO_4$. Phys Rev Lett. 2009; 103(3): 037004-037007. http://dx.doi.org/10.1103/PhysRevLett.103.037004

[37] Inosov DS, Park JT, Charnukha A, Li Y, Boris AV, Keimer B *et al*. A crossover from weak to strong pairing in unconventional superconductors. Arxiv: 1012.4041v1 [cond-mat.supr-con] 18 Dec 2010.

[38] Sato T, Kamiyama T, Takahashi T, Kurahashi K and Yamada K. Observation of -like superconducting gap in an electron-doped high-temperature superconductor Science 2001; 291(5508): 1517-1519. http://dx.doi.org/10.1126/science.1058021

[39] Dagan Y, Beck R and Greene RL. Dirty Superconductivity in the Electron-Doped Cuprate $Pr_{2-x}Ce_xCuO_{4-\delta}$. Tunneling Study. Phys Rev 2007; 99(14): 147004-04.

[40] Matsui H, Terashima K, Sato T, Takahashi T, Fujita M, and Yamada K. Direct Observation of a Nonmonotonic - Wave Superconducting Gap in the Electron- Doped High-Superconductor $Pr_{0.89}LaCe_{0.11}CuO_4$. Phys Rev Lett 2005; 95(1): 017003(4pages).

[41] Giubileo F, Piano S, Scarfato A, Bobba F, Bartolomeo AD and Cucolo AM. A tunneling spectroscopy study of the pairing symmetry in the electron-doped $Pr_{1-x}LaCe_xCuO_{4-y}$. J Phys Condens Matter 2010; 22(4) 045702. http://dx.doi.org/10.1088/0953-8984/22/4/045702

[42] Niestemski FC, Kunwar S, Zhou S, Li S, Ding H, Z. Wang Z, P. Dai P, and Madhavan V, A distinct bosonic mode in an electron-doped high- transition-temperature superconductor. Nature (London) 2007; 450(7172): 1058-1061. http://dx.doi.org/10.1038/nature06430

[43] Shan L, Huang Y, Wang YL, Li S, Zhao J, Dai P, Zhang YZ, Ren C, and Wen HH. Weak-coupling Bardeen-Cooper-Schrieffer superconductivity in the electron-doped cuprate superconductors. Phys Rev B 2008; 77 (1): 014526-5. http://dx.doi.org/10.1103/PhysRevB.77.014526

[44] Brandaw B. Characteristic features of the exotic superconductors. Phys Rep 1998; 296(1): 1-63. http://dx.doi.org/10.1016/S0370-1573(97)00071-9

[45] Welp U, Kwok WK, Crabtree GW, Vandervoort KG and Liu JZ.Magnetic measurements of the upper critical field of $YBa_2Cu_3O_{7-\delta}$ single crystals. Phys Rev Lett 1989; 62(16): 1908-1911. http://dx.doi.org/10.1103/PhysRevLett.62.1908

[46] Hao Z, Clem JR, McElfresh MW, Civale L, Malozemoff AP and Holtzberg F. Model for the reversible magnetization of high-κ type-II superconductors: Application to high-superconductors. Phys Rev B 1991; 43(4): 2844-2852. http://dx.doi.org/10.1103/PhysRevB.43.2844

[47] Brandsatter G, Sauerzopf FM, Weber HW, Ladenberger F and Schwarzmann E. Upper critical field, penetration depth, and GL parameter of Tl-2223 single crystals. Physica C 1994; 235-240(3): 1845-1846.

[48] Li Q, Suenaga M, Hikata T and Sato K. Two-dimensional fluctuations in the magnetization of $Bi_2Sr_2Ca_2Cu_3O_{10}$. Phys Rev B 1992; 46(9): 5857-5860. http://dx.doi.org/10.1103/PhysRevB.46.5857

[49] Batlogg B, Kourouklis G, Weber W, Cava RG, Jayaraman A, White AE *et al*. Nonzero isotope effect in $La_{1.85}Sr_{0.15}CuO_4$. Phys. Rev. Lett 1987; 59(8): 912-918. http://dx.doi.org/10.1103/PhysRevLett.59.912

[50] Batlogg B, Cava RJ, Jayaraman A, van Dover RB, Kourouklis GA, Sunshine S *et al*. Isotope effect in the high-superconductors $Ba_2YCu_3O_7$ and $Ba_2EuCu_3O_7$. Phys Rev Lett 1987; 58(22) 2333-2336. http://dx.doi.org/10.1103/PhysRevLett.58.2333

[51] Katayama-Yoshida H, Hirooka T, Oyamada A, Okabe Y, Takahashi T, Sasaki T, *et al*. Oxygen isotope effect in the superconducting Bi-Sr-Ca-Cu-O system. Physica C 1989; 156(3): 481-484. http://dx.doi.org/10.1016/0921-4534(88)90776-9

[52] Franck JP, Harker S and Brewer JH. Copper and oxygen isotope effects in $La_{2-x}Sr_xCuO_4$. Phys Rev Lett 1993; 71(2): 283-286. http://dx.doi.org/10.1103/PhysRevLett.71.283

[53] Crawford MK, Farneth WE, McCarron EM, III, Harlow RL and Moudden AH. Oxygen isotope effect and structural phase transitions in La_2CuO_4-based superconductors Science 1990; 250(4986): 1390-1393. http://dx.doi.org/10.1126/science.250.4986.1390

[54] Franck JP, Jung J, Mohamed MAK, Gygax S and Sproule GI. Observation of an oxygen isotope effect in superconducting $(Y_{1-x}Pr_x)Ba_2Cu_3O_{7-\delta}$. Phys Rev B 1991; 44(10): 5318-5321. http://dx.doi.org/10.1103/PhysRevB.44.5318

[55] Kulé ML. Importance of the electron-phonon interaction with the forward scattering peak for superconducting pairing in cuprates. J Supercond Novel Magnetism 2006; 19(3-5): 213-249.

[56] Bishop AR, Bussmann-Holder A, Doglov OV, Furrer A, Kamimura H, Keller H *et al*. Real and marginal Isotope Effects in Cuprates Superconductors. J Supercond Nov Magn 2007; 20(5): 393-396. http://dx.doi.org/10.1007/s10948-007-0235-6

[57] Batlogg B. A critical review of selected experiments in high-Tc superconductivity Physica B 1991; 169(1-4): 7-16. http://dx.doi.org/10.1016/0921-4526(91)90201-O

[58] Hidaka Y and Suzuki M. Growth and anisotropic superconducting properties of $Nd_{2-x}Ce_xCuO_{4-y}$ single crystals. Nature 1989; 338(6217): 635-637 http://dx.doi.org/10.1038/338635a0

[59] Machkenzie AP, Julian SR, Sinclair DC and Lin CT. Normal-state magnetotransport in superconducting $Tl_2Ba_2CuO_{6+\delta}$ to millikelvin temperatures. Phys Rev B 1996; 53(9): 5848-5855. http://dx.doi.org/10.1103/PhysRevB.53.5848

[60] Takenaka K, Mizuhashi K, Takagi H, and Uchida S. Interplane charge transport in $YBa_2Cu_3O_{7-y}$: Spin-gap effect on in-plane and out-of-plane resistivity Phys Rev B 1994; 50(9): 6534-6527. http://dx.doi.org/10.1103/PhysRevB.50.6534

[61] Markiewicz RS. A survey of the van Hove scenario for high-superconductivity with special emphasis on pseudogap and striped phases. J Phys Chem Solids 1997; 58(8): 1179-1310. http://dx.doi.org/10.1016/S0022-3697(97)00025-5

[62] Pattnaik PC, Kane CL. Newns DM. Tsuei CC. Evidence for the van Hove scenario in high-temperature superconductivity from quasiparticle-life time broadening. Phys Rev B 1992; 45(10): 5714-5717. http://dx.doi.org/10.1103/PhysRevB.45.5714

[63] Lu DH, Schmidt M, Cummuns TR, Schuppler S, Lichtenberg F and Bednorz JG. Fermi Surface and Extended van Hove Singularity in the Noncuprate Superconductor Sr_2RuO_4 Phys Rev Lett 1996; 76(25): 4845-4848. http://dx.doi.org/10.1103/PhysRevLett.76.4845

[64] Hellman ES. Umklapp electron-electron scattering resistivity of half-filled copper-oxygen chains and planes. Phys Rev B 1989; 39(13): 9604-9606. http://dx.doi.org/10.1103/PhysRevB.39.9604

[65] Tsuei CC, Gupta A, Koren G. High-resolution angle-resolved photoemission study of the Fermi surface and the normal-state electronic structure of $Bi_2Sr_2CaCu_2O_8$. Physica C 1989; 161(3): 415-422. http://dx.doi.org/10.1016/0921-4534(89)90354-7

[66] Kubo Y, Shimakawa Y, Manako T, Igarashi H. Transport and magnetic properties of $Tl_2Ba_2CuO_{6+\delta}$ showing a δ-dependent gradual transition from an 85-K superconductor to a nonsuperconducting metal. Phys Rev B 1991; 43(10): 7875-7882. http://dx.doi.org/10.1103/PhysRevB.43.7875

[67] Newns DM, Tsuei CC, Huebener RP, van Pentum PJM, Pattnaik PC and Chi CC. Quasiclassical transport at a van Hove singularity in cuprate superconductors. Phys Rev Lett 1994; 73(12): 1695-1698. http://dx.doi.org/10.1103/PhysRevLett.73.1695

[68] Dessau DS, Shen Z-X, King DM, Marshall DS, Lombardo LW, Dickinson PH *et al*. Key features in the measured band structure of $Bi_2Sr_2CaCu_2O_{8+\delta}$: Flat bands at E_F and Fermi surface nesting. Phys Rev Lett 1993; 71(17): 2781-2784. http://dx.doi.org/10.1103/PhysRevLett.71.2781

[69] Olson CG, Liu R, Lynch DW, List RS, Arko AJ, Veal BW *et al*. Phys Rev B. High- resolution angle-resolved photoemission study of the Fermi surface and the normal-state electronic structure of $Bi_2Sr_2CaCu_2O_8$ 1990; 42(1); 381-386.

[70] Hwang HY, Batlogg B, Takagi H, Kao HL, Kav RJ, Krajewski JJ, *et al*. Scaling of the temperature dependent Hall effect in $La_{2-x}Sr_xCuO_4$ Phys Rev Lett 1994; 72(16): 2636-2639. http://dx.doi.org/10.1103/PhysRevLett.72.2636

[71] Ino A, Kim C, Nakamura M, Yoshida T, Mizokawa T, Fujimori A *et al*. Doping-dependent evolution of the electronic structure of $La_{2-x}Sr_xCuO_4$ in the superconducting and metallic phases. Phys Rev B. 2002; 65(9): 094504-11. http://dx.doi.org/10.1103/PhysRevB.65.094504

[72] Blumberg G, Stojković BP and Klei MV. Aniferromagnetic excitations and van Hove singularities in $YBa_2Cu_3O_{6+x}$. Phys Rev B 1995; 52(22): R15741-R15744. http://dx.doi.org/10.1103/PhysRevB.52.R15741

[73] Moca CP, Tifrea I and Crisan M. An analytical approach for the pseudogap in the spin fluctuations model. J Supercond Incorp Novel Mag. 2000; 13(3): 411-416.

[74] Chaudhuri I, Taraphder A and Ghatak SK. Pseudogap and its influence on normal And superconducting states of cuprates. Physica C 2001; 353(1-2): 49-59. http://dx.doi.org/10.1016/S0921-4534(00)01743-3

[75] Borne AJH, Carbotte JP and Nicol EJ. Signature of pseudogap formation in the density of states of underdoped cuprates. arxiv: 1006.3232v1[cond-mat.supr-con] 16 Juin 2010.

[76] Vaknin D, Sinha SK, Moncton DE, Johnston DC, Newsam JM, Safinya CR, *et al*, Antiferromagnetism in La_2CuO_{4-y}. Phys Rev Lett 1987; 58(26): 2802-2805. http://dx.doi.org/10.1103/PhysRevLett.58.2802

[77] Keimer B, Aharony A, Auerbach A, Birgeneau RJ, Cassanho A, Endoh Y *et al*. Néel transition and sublattice magnetization of pure and doped La_2CuO_4 Phys Rev B 1992; 45(13): 7430-7435. http://dx.doi.org/10.1103/PhysRevB.45.7430

[78] Hayden SM, Aeppli G, Perring TG, Mook HA, and Dogan F. High-frequency spin waves in $YBa_2Cu_3O_6$.15. Phys Rev B 1996; 54(10): R6905-R6908. http://dx.doi.org/10.1103/PhysRevB.54.R6905

[79] Mizuki J, Kubo Y, Manako T, Shimakawa Y, Igarashi H Tranquada JM *et al.* Antiferromagnetism in $TlBa_2YCu_2O_7$. Physica C 1988; 186(5): 781-784. http://dx.doi.org/10.1016/0921-4534(88)90159-1

[80] Vaknin D, Caignol E, Davies PK, Fisher JE, Johnston DC, and Goshorn DP. Antiferromagnetism in $(Ca_{0.85}Sr_{0.15})$ CuO_2, the parent of the cuprate family of superconducting compounds Phys Rev B 1989; 39(13): 9122-9125. http://dx.doi.org/10.1103/PhysRevB.39.9122

[81] Matsuda M, Yamaka K, Kakurai K, Kadowaki H, Thurston TR, Endoh Y, *et al.* Three-dimensional magnetic structures and rare-earth magnetic ordering in Nd_2CuO_4 and Pr_2CuO_4. Phys Rev B 1990; 42(16): 10098-10107. http://dx.doi.org/10.1103/PhysRevB.42.10098

[82] Bourges P, Casalta H, Ivanov AS, and Petitgrand D. Superexchange Coupling and Spi Susceptibility Spectral Weight in Undoped Monolayer Cuprates. Phys Rev Lett 1997; 79(24): 4906-4909. http://dx.doi.org/10.1103/PhysRevLett.79.4906

[83] Sumarli IW, Lynn JW, Chattopadhyay T, Barilo SN, Zhugonov DI, and Peng JL. Magnetic structure and spin dynamics of the Pr and Cu in Pr_2CuO_4. Phys Rev B 1995; 51(9): 5824-5839. http://dx.doi.org/10.1103/PhysRevB.51.5824

[84] Hayden FM, Aeppli G, H. Mook HA, Perring TG, Mason TE, SW. Cheong, *et al.* Comparison of the high-frequency magnetic fluctuations in insulating and Superconducting $La_{2-x}Sr_xCuO_4$. Phys Rev Lett 1996; 76(8): 1344-1347. http://dx.doi.org/10.1103/PhysRevLett.76.1344

[85] Birgeneau RJ, Gabbe DR, Jenssen HP, Kastner MA, Picone PJ, Thurston TR, *et al*. Antiferromagnetic spin correlations in insulating, metallic, and superconducting $La_{2-x}Sr_xCuO_4$. Phys Rev B 1988; 38(10): 6614-6623. http://dx.doi.org/10.1103/PhysRevB.38.6614

[86] Rigamonti A, Borsa F, Corti M, Rega T, Ziolo J and Waldner F. Magnetic correlations and spin dynamics in $La_{2-x}Sr_xCuO_4$ from NQR relaxation. Earlier and Recent Aspects of Superconductivity, edited by Bednorz JG and Müller KA 1991; 441-466.

[87] Keimer B, Birgeneau RJ, Cassanho A, Endoh Y, Erwin RW, Kastner MA, *et al*. Scaling Behavior of the Generalized Susceptibility in $La_{2-x}Sr_xCuO_{4+y}$. Phys Rev Lett 1991; 67(14): 1930-1933. http://dx.doi.org/10.1103/PhysRevLett.67.1930

[88] Rossat-Mignot, Bourges P, Onufrieva F, Regnault LP, J.Y. Henry JY, Burlet P *et al*. Spin dynamics in the high- system $YBa_2Cu_3O_{6+x}$: the heavily doped regime. Physica B 1994; 199-200(1): 281-283.

[89] Regnault LP, Bourges P, Burlet P, Henry JY, Rossat-Mignod J *et al*. Spin dynamics in the normal and superconducting states of $YBa_2Cu_3O_{6+x}$. physica C 1994; 235-240(P1): 59-62.

[90] Warren WW, Waldstedt Re, Brennert GF, Cava RJ, Tycko R, Bell RF *et al.* Cu spin dynamics and superconducting precursor effects in planes above in $YBa_2Cu_3O_{6.7}$. Phys Rev Lett 1989; 62(10): 1193-1196. http://dx.doi.org/10.1103/PhysRevLett.62.1193

[91] Birgeneau RJ, Endoh Y, Kakurai K, Hidaka Y, Murakami T, Kastner MA *et al*. Static and dynamic spin fluctuations in superconducting $La_{2-x}Sr_xCuO_4$. Phys Rev B 1989; 39(4): 2868-2871. http://dx.doi.org/10.1103/PhysRevB.39.2868

[92] Oda M, Matsaki H and Ido M. Common features of magnetic and superconducting properties in Y-doped $Bi_2(Sr,Ca)_3Cu_2O_8$ and Ba(Sr)-doped La2CuO4 Solid State Commun. 1990; 74(12) 1321-1326. http://dx.doi.org/10.1016/0038-1098(90)91000-7

[93] Birgeneau RJ, Greven M, Kastner MA, Lee YS, Wells BO, Endoh Y *et al*. Instantaneous spin correlations in La_2CuO_4. Phys Rev B 1999; 59(21): 13788-13794. http://dx.doi.org/10.1103/PhysRevB.59.13788

[94] Tranquada JM. Neutron Scattering Studies of Aniferromagnetic correlations in Cuprates. Hand Book of High-Temperature Superconductivity. Theory and Experiment, edited by John Robert Shrieffer. 257-298.

[95] Chakravarty S, Halperin BI, and Nelson DR. Two-dimensional quantum Heisenberg antiferromagnet at low temperatures. Phys Rev B 1989; 39 (4): 2344-2371. http://dx.doi.org/10.1103/PhysRevB.39.2344

[96] Hasenfratz P and Niedermayer F. The exact correlation length of the antiferromagnetic d=2+1 Heisenberg model at low temperatures. Phys Lett B 1991; 268(2): 231-235 http://dx.doi.org/10.1016/0370-2693(91)90809-5

[97] Barford W and Gunn JMF. The theory of the measurement of the London penetration depth in uniaxial type II superconductors by muon spin rotation. Physica C 1988; 156(4): 515-522. http://dx.doi.org/10.1016/0921-4534(88)90014-7

[98] Schneider T and Frick. Experimental constraints and theory of layered high-temperature superconductors. Earlier and Recent Aspects of Superconductivity, edited by Bednorz JG and Müller KA. 1991; 501-517.

[99] Keller H. Muon spin rotation experiments in high-superconductors. Earlier and Recent Aspects of Superconductivity, edited by Bednorz JG and Müller KA 1991; 222-239.

[100] Harshman DR, Schneemeyer LF, Vaszczak JV, Aeppli G, Cava RJ, Batlogg B, *et al*. Magnetic penetration depth in single-crystal $YBa_2Cu_3O_{7-\delta}$. Phys Rev B 1989; 39(1): R851-R854. http://dx.doi.org/10.1103/PhysRevB.39.851

[101] Fruchter R, Giovannella C, Collin G, and Campbell IA. Lower critical fields and pinning in $YBa_2Cu_3O_{7-\delta}$. Physica C 1988; 156(1): 69-72. http://dx.doi.org/10.1016/0921-4534(88)90107-4

[102] Fiory AT, Hebard AF, Mankiewich PM, and Hoard RE.Renormalization of the mean-field superconducting penetration depth in epitaxial $YBa_2Cu_3O_7$ Films. Phys Rev Lett.1988; 61(12): 1419-1422. http://dx.doi.org/10.1103/PhysRevLett.61.1419

[103] Krusin-Elbaum L, Greene RL, Holtzberg F, Malozemoff AP and Yeshurun Y. Direct Measurement of the Temperature Dependent Magnetic Penetration Depth in Y-Ba-Cu-O Crystals. Phys Rev Lett 1989; 62(2): 217-220. http://dx.doi.org/10.1103/PhysRevLett.62.217

[104] Krusin-Elbaum L, Malozemoff AP, Malozemoff AP, Cronemeyer DC and Holtzberg F. Temperature dependence of lower critical fields in Y-Ba-Cu-O crystals. Phys Rev B

1989; 39(4): 2936-2939.
http://dx.doi.org/10.1103/PhysRevB.39.2936

[105] Scheidt E-W, Huch C, Luders K and Muller V. Magnetic penetration depth in oriented YBaCuO powder samples. Solid State commun 1989; 71(6): 505-509.
http://dx.doi.org/10.1016/0038-1098(89)90101-4

[106] Bechlaghem A, Properties of the Coherence Length and van Hove Singularity in High- Superconductors. Int J App Phys Res 2015: 2(1): 19-30.
http://dx.doi.org/10.15379/2408-977X.2015.02.01.3

[107] Zhou XJ, Cuk T, Devereaux T, Nagaosa N, Shen Z-X. Angle-Resolved Photoemission Spectroscopy on electronic Structure and Electron- Phonon Coupling in Cuprate Superconductors. HandBook of High-Temperature Superconductivity. Theory and Experiment, edited by John Robert Shrieffer. 87-144.

[108] Xing DY, Liu M and Gong CD. Comment on "Anomalous isotope effect and van Hove singularity in superconducting Cu oxides". Phys Rev Lett 1992; 68(7): 1090.
http://dx.doi.org/10.1103/PhysRevLett.68.1090

[109] Schulz HJ. Superconductivity and antiferromagnetism in the two-dimensional Hubbard model: Scaling theory. Europhys Lett 1987; 4(5): 609-615.
http://dx.doi.org/10.1209/0295-5075/4/5/016

[110] Yndurain F. Model for the variation upon doping of the isotope coefficient in high- superconductors. Phys Rev B 1995; 51(13): 8495-8497.
http://dx.doi.org/10.1103/PhysRevB.51.8494

[111] Croft TP, Lester C, Senn MS, Bombardi A and Hayden SM. Charge density wave fluctuations in $La_{2-x}Sr_xCuO_4$ and their competition with superconductivity. Phys Rev B 2014; 89(22): 224513-20.
http://dx.doi.org/10.1103/PhysRevB.89.224513

[112] Torchinsky DH, Mahmood F, Bollinger AT, Božović I and Gedik N. Competition of superconductivityand charge Density Wave inCuprates: Recent evidence and interpretation. Nature Materials 2013; 12(1) 387-391.
http://dx.doi.org/10.1038/nmat3571

[113] Chang J, Blackburn E, Holmes AT, Christensen NB, Larsen J, Mesot J *et al*. Direct observation of competition between superconductivity and charge density wave order in $YBa_2Cu_3O_{6.67}$. Nature Phys. 2012; 8(1): 871-876.
http://dx.doi.org/10.1038/nphys2456

[114] Cappelluti E and Pietronero L. Nonadiabatic superconductivity: The role of van Hove singularities. Phys. Rev B 1996; 53(2): 932-944.
http://dx.doi.org/10.1103/PhysRevB.53.932

[115] Shen Z-X, Spicer WE, King DM, Dessau DS, Wells BO. *et al*. Photoemission Studie of High- Superconductors: The superconducting gap. Science. 1995; 267(5196343-350.

[116] Kresin VS, Wolf SA. Major normal and superconducting parameters of high- oxides. Phys Rev B 1990; 41(7): 4278-4285.
http://dx.doi.org/10.1103/PhysRevB.41.4278

[117] Kresin VZ and Wolf SA and Ovchinnikov. Exotic normal and superconducting properties of the high- oxides. Physics Reports 1997; 288(1-6): 347-354.
http://dx.doi.org/10.1016/S0370-1573(97)00032-X

[118] Bouvier J and Bok J. Gap anisotropy and van Hove singularties in high superconductors. Physica C 1997; 249(1): 117-122.

[119] Kato K. New interpretation of the role of electron–phonon interactions in electron pairing in superconductivity. Synthetic Metals 2013; 181: 45-51.
http://dx.doi.org/10.1016/j.synthmet.2013.07.025

[120] Muller KA. From Single- to Bipolarons with Jahn-Teller Character and Metallic Cluster-Stripes in Hole-Doped Cuprates, edited by John Robert Shrieffer 2006; 399-425.

[121] Apostol M. On the mechanism of high-temperature superconductivity in Ba-La(Y)-Cu-O type systems. Int J Mod Phys B 1987; 1(3-4): 957-964.
http://dx.doi.org/10.1142/S0217979287001377

[122] Apostol M and Popescu M. The relation between the critical temperature and the oxygen content of the superconducting phase YBa_2Cu_3Oz. Phyl Mag Lett 1988; 57(6): 305-309.
http://dx.doi.org/10.1080/09500838808214718

[123] Liu FH and Apostol M. Critical temperature, isotope effect and superconducting gap in the $M_xLa_{2-x}CuO_4$ and $M_2RCu_3O_{7-\delta}$-type superconductors. Int J Mod Phys B 1988; 2(6): 1415-1429.
http://dx.doi.org/10.1142/S0217979288001256

[124] Apostol M. On the high temperature superconductivity in 123-class of superconductors. Mod Phys Lett B. 1989; 3(11) 847-852.
http://dx.doi.org/10.1142/S0217984989001333

[125] Vasiliu L and Apostol M. On the high-temperature superconductivity of $Sr_xLa_{2-x}CuO_{4-\delta}$. J Supercond 1989; 2(4) 513-528.
http://dx.doi.org/10.1007/BF00627564

[126] Apostol M, Buzatu F and Liu FH. Critical temperature of third generation high-temperature superconductors. Int J Mod Phys B. 1990; 4(1): 159-177.
http://dx.doi.org/10.1142/S0217979290000103

[127] Friedel. Electron-Phonon Interactions and Phase Transition.Edited by Riste T (Plenum, N, Y, 1977: 1.

[128] Markiewicz RS. Van Hove excitons and high-superconductivity VIIIB. vHs - Jahn-Teller effect. Physica C 1992; 200(1-2): 65-91.
http://dx.doi.org/10.1016/0921-4534(92)90323-5

[129] Markiewicz RS. Van Hove Excitons and High-Superconductivity: VIIIC Dynamic Jahn-Teller Effects vs Spin-Orbit Coupling in the LTO Phase of $La_{2-x}Sr_xCuO_4$. ArXiv: cond. Mat/9303020v1. 3 Mar 1993.

[130] Markiewicz RS. Van Hove Jahn-Teller effect and high-superconductivity. J Physics and Chemestry of Solids. 1993; 54(10): 1153-1156
http://dx.doi.org/10.1016/0022-3697(93)90158-N

[131] Bardeen J, Cooper LN and Schrieffer JR. Theory of superconductivity. Phys Rev 1957; 108: 1175-1204.
http://dx.doi.org/10.1103/PhysRev.108.1175

[132] Bechlaghem A and Bourbie D. Theory of the isotope effect and superconducting transition temperature in High- Oxides. Mod Phys Lett B 2011; 25(26): 2069-2078.
http://dx.doi.org/10.1142/S0217984911027248

[133] Bechlaghem A, Mostéfa and Zanoun Y. Gap energy, Isotope Effect and Coherence Length in High- Oxides. Int J Mod Phys B 1999; 13(22): 3915-3925.
http://dx.doi.org/10.1142/S0217979299004082

[134] Force L and Bok J. Solid State Commun. Superconductivity in two dimensional systems: van Hove singularity and Coulomb repulsion. Solid State Commun 1993; 85(11): 975-978.
http://dx.doi.org/10.1016/0038-1098(93)90716-Z

[135] Tsuei CC, Newns DM, Chi CC and Pattnaik PC. Anomalous Isotope Effect and van Hove Singularity in Superconducting Cu Oxides. Phys Rev Lett 1990; 65(21): 2724- 2727.
http://dx.doi.org/10.1103/PhysRevLett.65.2724

[136] Szczesniak R, Mierzejewski M, Zielinski J and Entel P. Modification of the isotope effect by the van Hove singularity of electrons on a two-dimensional lattice. Sold State Commun 2001; 117(1): 369-371.
http://dx.doi.org/10.1016/S0038-1098(00)00477-4

[137] Bechlaghem A and Bourbie D. Properties of the superconducting Gap Ratio in the Van Hove Scenario of High- Oxides. Mod Phys Lett B 2010; 24(23): 2395-2401.
http://dx.doi.org/10.1142/S0217984910024638

[138] Loeser AG, Shen Z-X, Dessau DS, Marshall DS, Park CH, Fournier P, *et al*. Excitation gap in the normal state of underdoped Bi2Sr$_2$CaCu$_2$O$_{8+\delta}$. Science 1996; 273(5273): 325-329. http://dx.doi.org/10.1126/science.273.5273.325

[139] Shen Z-X, Spicer WE, King DM, Dessau DS, Wells BO, *et al*. Photoemission studies of high- superconductors: The superconducting gap. Science 1995; 267(5196) 343-350. http://dx.doi.org/10.1126/science.267.5196.343

[140] Williams GVM, Tallon JL, Haines EM, Michalak R, and Dupree R. NMR evidence for a d-wave normal-state pseudogap. Phys Rev Lett 1997; 78(4): 721-724. http://dx.doi.org/10.1103/PhysRevLett.78.721

[141] Williams GVM, Haines EM, and Tallon JL. Pair breaking in the presence of a normal-state pseudogap in high- cuprates. Phys Rev B 1998; 57(1): 146-149. http://dx.doi.org/10.1103/PhysRevB.57.146

[142] Tsuei CC, Kirtley JR, Chi CC, Yu-Jahnes LS, Gupta A, Shaw A, *et al*. Pairing symmetry and flux quantization in a tricrystal superconducting ring of YBa$_2$Cu$_3$O$_{7-\delta}$. Phys Rev Lett. 1994; 73(4): 593-596. http://dx.doi.org/10.1103/PhysRevLett.73.593

[143] Khasanov R, Shengelaya A, Maisuradze A, La Mattina F, Bussmann-Holder A, Keller H *et al*. Experimental evidence for two gaps in the high-temperature La$_{1.83}$Sr$_{0.17}$CuO$_4$ superconductor. Phys Rev Lett 2007; 98(5): 057007-4. http://dx.doi.org/10.1103/PhysRevLett.98.057007

[144] Deutscher G. Andreev–Saint-James reflections: A probe of cuprate superconductors. Rev Mod Phys 2005; 77(1): 109-135. http://dx.doi.org/10.1103/RevModPhys.77.109

[145] Loeser AG, Dessau DS and Shen ZH. Doping dependence of Bi$_2$Sr$_2$CaCu$_2$O$_{8+\sigma}$ in the normal state. Physica C 1996; 263(1-4); 208-213. http://dx.doi.org/10.1016/0921-4534(96)00074-3

[146] Marshal DS, Dessau DS, Loeser AG, Park CH, Matsuura AY, Eckstein JN *et al*. Unconventional Electronic Structure Evolution with Hole Doping in Bi$_2$Sr$_2$CaCu$_2$O$_{8+\delta}$: Angle-Resolved Photoemission Results. Phys Rev Lett 1996; 76(25): 4841-4844 http://dx.doi.org/10.1103/PhysRevLett.76.4841

[147] Ding H, Yokowa T, Campuzano JC, Takahashi T, Randeria M, norman MR *et al*. Spectroscopic evidence for a pseudogap in the normal state of underdoped high-Tc superconductors Nature 1996; 382(6586): 51-54. http://dx.doi.org/10.1038/382051a0

[148] Sherman A and Schreiber M. Normal-state pseudogap in spectrum of strongly correlated frmions. Phys Rev B 1997; 55(2): R712-R715. http://dx.doi.org/10.1103/PhysRevB.55.R712

[149] Houssa M, Ausloos M and Cloots R. Thermal conductivity of YBa$_2$(Cu$_{1-x}$Zn$_x$)O$_{7-\delta}$: Relation between x and δ. Phys Rev B 1997; 56(10): 6226-6230. http://dx.doi.org/10.1103/PhysRevB.56.6226

[150] Bechlaghem A. Fundamental Properties and Origin of the High-Tc Cuprate Superconductors: Development of Concepts. Int J Adv App Phys Res 2014; 1(1): 19- 34. http://dx.doi.org/10.15379/2408-977X.2014.01.01.3

[151] Dai P, Mook HA and Dogan F. Pseudogap and incommensurate magnetic fluctuations in YBa$_2$Cu$_3$O$_{6.6}$. Physica B. 1998; 241-213: 524-523.

[152] Bouvier J and Bok J. Van Hove Singularity and "Pseudogap" in HTSC. J of supercond. 1997; 10(6): 673-676. http://dx.doi.org/10.1007/BF02471931

[153] Rossat-Mignod J, Regnault LP, Vettier C, Bourges P, Burlet P, Bossy J, *et al*. Neutron scattering study of the YBa$_2$Cu$_3$O$_{6+x}$ system. Physica C 1991; 185-189 (1): 86-92. http://dx.doi.org/10.1016/0921-4534(91)91955-4

[154] Panda SK, Rout GC. Interplay of CDW, SDW and superconductivity in high- cuprates. Physica C 2009; 469(13): 702-706. http://dx.doi.org/10.1016/j.physc.2009.03.005

[155] Hücker M, Christensen NB, Holmes AT, Blackburn E, Forgan EM, Liang R. Competing charge, spin, and superconducting orders in underdoped YBa$_2$Cu$_3$O$_y$. ArXiv: 1405. 7001.v1 [cond. Mat.supr-con] 17 May 2014.

[156] Getino JM. De Llano M and Rbio H. Properties of the gap energy in the van Have scenario of high-temperature superconductivity. Phys Rev B 1993; 48(1): 597-599. http://dx.doi.org/10.1103/PhysRevB.48.597

[157] Gupta HC. Electron-phonon interaction for an analytic solution to the BCS equation for the high temperature superconductors. Mod Phys Lett B 1991; 5(20): 1349-1353. http://dx.doi.org/10.1142/S0217984991001647

[158] Bouvier J and Bok J. Gap anisotropy and van Hove singularities in high superconductors. Physica C. 1995; 249(1): 117-122. http://dx.doi.org/10.1016/0921-4534(95)00294-4

[159] Ratanaburi S, Udomsamuthirun P and Yoksan S. Ratio in a van Hove superconductor. J Supercond 1996; 9(5): 485-486. http://dx.doi.org/10.1007/BF00723519

[160] Krunavakarn B, Udomsamuthirun P, Yoksan S, Grosu I and Crisan M. The gap-to- ratio of a van Hove superconductor. J Supercond 1998; 11(2): 271-273. http://dx.doi.org/10.1023/A:1022636001976

[161] Pakokthom C, Krunavakarn B, Udomsamuthirun P and Yoksan S. Reduced-gap ratio of high- cuprates within the d-wave two-dimensional van Hove scenario. J Supercond 1998; 11(4): 429-432. http://dx.doi.org/10.1023/A:1022645630932

[162] Kaskamalas S, Krunavakarn B, Rungruang P and Yoksan S. Dependence of the gap ratio on the Fermi level shift in a van Hove superconductor. J Supercond Incorp Novel Mag. 2000; 13(1): 33-36. http://dx.doi.org/10.1142/s0217979200002387

[163] Sarkar S and Das AN. Isotope-shift exponent, pressure coefficient of, and the superconducting-gap ratio within the van Have scenario. Phys Rev B. 1994; 49(18): 13070-5. http://dx.doi.org/10.1103/PhysRevB.49.13070

[164] Das AN, Lahiri J and Sil S. Superconducting gap ratio and isotope-shift exponent in a pair-tunneling model. Physica C 1998; 294(1-2): 97-104. http://dx.doi.org/10.1016/S0921-4534(97)01754-1

[165] Szczesniak R and Dyga M. The van Hove singularity and two-dimensional charge Density waves. Exact analytical results. Acta Physica Slovaca 2003; 53(6): 477-487.

[166] Gabovich AM, Voitenko AI, Ekino T, Li MS, Szymczak H and Pekała M. Competition of superconductivity and charge density waves in cuprates: Recent evidence and interpretation. Advances in Condensed Matter Physics 2009; 2010(1): 681070-109.

[167] Orozco S, Ortiz MA, Méndez-Moreno RM and Mreno M. A model of the isotope effect in high- superconductors. Physica C 2004; 408-410: 346-347. http://dx.doi.org/10.1016/j.physc.2004.02.102

[168] Shneyder EI and Ovchinnikov SG. Isotope Effect in the Model of Strongly Correlated Electrons with the Magnetic and Phonon superconducting Pairing Mechanisms. Journal of Experimental and theoretical Physics JETP 2009; 109(6): 1017-1021. http://dx.doi.org/10.1134/S1063776109120139

[169] Bill B and Kresin VZ. Isotope Effect in High- Superconductors due to Non-Adiabaticity, Proximity Effect and Magnetic Impurties. Zeitschrift fur Physikalishe Chemie Bd 1997; 201, S: 271-284.

[170] Bill B and Kresin VZ. Isotope Effect in High- Materials: Role of non adiabicity and magnetic imurties. Z Phys B. 1997;

104(4): 759-763.
http://dx.doi.org/10.1007/s002570050523

[171] Balseiro CA and Falicov LM. Superconductivity and charge-density waves. Phys Rev B 1979; 20(11): 4457-4464.
http://dx.doi.org/10.1103/PhysRevB.20.4457

[172] Muller KA, Nature (London). Possible coexistence of - and - wave condensates in copper oxide superconductors. Naure (London) 1995; 377(6545): 133-135.
http://dx.doi.org/10.1038/377133a0

[173] Muller KA and. Keller H, High-Tc Superconductivity1996: Ten YearsafterDiscovery (Kluwer Academic,Dordrecht, 1997), p. 7.

[174] Khasanov R, Shengelaya A, Maisuradze A, La Mattina F, Bussmann-Holder A and Keller H. Experimental Evidence for Two Gaps in the High-Temperature $La_{0.83}Sr_{0.17}CuO_4$ Superconductors. Phys Rev Lett 2007: 98: 057007-04.
http://dx.doi.org/10.1103/PhysRevLett.98.057007

[175] Lu YM, Xiang T and Lee DH. Underdoped superconducting cuprates as topological superconductors. Nature Physics. 2014; 10: 634-637.
http://dx.doi.org/10.1038/nphys3021

[176] Sacks W, Mauger A and Yves Noat Y. Mean-field approach to unconventional superconductivity. Physica C. 2014; 503(8): 14-24.
http://dx.doi.org/10.1016/j.physc.2014.04.041

[177] Szczesniak R, Jarosik MW, and Duda AM. The Correlation between the Energy Gap and the PseudogapTemperature in Cuprates: The YCBCZO and LSHCO Case. Advances in Condensed Matter Physics. 2015; 2015: 10 pages

Received on 27-11-2015 Accepted on 25-12-2015 Published on 28-01-2016

http://dx.doi.org/10.15379/2408-977X.2016.03

© 2016 A. Bechlaghem; Licensee Cosmos Scholars Publishing House.
This is an open access article licensed under the terms of the Creative Commons Attribution Non-Commercial License (http://creativecommons.org/licenses/by-nc/3.0/), which permits unrestricted, non-commercial use, distribution and reproduction in any medium, provided the work is properly cited.